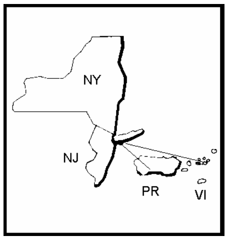

REGION 2
UNIVERSITY TRANSPORTATION RESEARCH CENTER

DEVELOPMENT OF SMART BRIDGE BEARINGS SYSTEM – A FEASIBILITY STUDY

Project # C-02-02

Final Report
December 2005

Submitted by:

Agrawal, A.K., Subramaniam, K. and Pan, Y.
Department of Civil Engineering
The City College of New York
New York, NY 10031

In cooperation with

University Transportation Research Center, Region 2
City College of New York

New York State Department of Transportation
and
U.S. Department of Transportation

MARSHAK HALL J910
THE CITY COLLEGE OF NEW YORK, NEW YORK 10031 212-650-8050 FAX 212-650-8374
WWW.UTRC2.ORG

DISCLAIMER STATEMENT

TECHNICAL REPORT
STANDARD TITLE PAGE

1. Report No. C-02-02	2.Government Accession No.	3. Recipient's Catalog No.
4. Title and Subtitle Development Of Smart Bridge Bearings System – A Feasibility Study Project # C-02-02		5. Report Date December 2005 6. Performing Organization Code
7. Author(s) A. K. Agrawal, The City College of New York K. Subramaniam, The City College of New York Y. Pan, The City College of New York		8. Performing Organization Report No.
9. Performing Organization Name and Address Region 2, University Transportation Research Center City College of New York, New York, NY 10031		10. Work Unit No. 11. Contract or Grant No. 55657-04-15
12. Sponsoring Agency Name and Address New York State Department of Transportation Albany, NY 12232	Federal Highway Administration U.S. Department of Transportation Washington, D.C.	13. Type of Report and Period Covered Final Report 14. Sponsoring Agency Code
15. Supplementary Notes		

16. Abstract

The goal of this project has been achieved through three tasks. The main goal of Task I has been to identify appropriate sensors that have potential for bridge bearings applications. This has been achieved through the following subtasks and has been presented in this chapter:

(a) An extensive literature review of behavior of elastomeric bearings and state-of-the-art on the smart bearings.

(b) Objective criteria for selection of sensors.

(c) Information, specifications and reliability of commercially advanced sensors.

The focus of Task II has been to develop possible instrumentation schemes for implementing smart bearings, as presented in Chapter 2. In Task III, costs associated with feasibility of smart bearings have been investigated. This work has been reported in Chapter 3.

17. Key Words Bridge bearings, smart bridges		18. Distribution Statement No restrictions	
19. Security Classif (of this report) Unclassified	20. Security Classif. (of this page) Unclassified	21. No of Pages 57	22. Price NA

Form DOT F 1700.7 (8-69)

ACKNOWLEDGMENTS

The research presented in this report was sponsored by New York State Department of Transportation (NYSDOT) through funds provided to the University Transportation Research Consortium (UTRC) at the City College of New York.

This research was jointly conducted by Professors Anil K. Agrawal (Principal Investigator) and Kolluru Subramaniam (Co-Principal Investigator). The investigators would like to thank NYSDOT for the financial support and assistance during the course of the project. Special thanks go to the members of the NYSDOT Task Working Group (TWG) and the Project Manager Mr. Jonathan Kunin. The investigators will also like to express their gratitude to Dr. Sreenivas Alampalli of the New York State Department of Transportation and Dr. Mohammed Ettouney for their comments and suggestions during the course of this project. Continuous support by Professor Robert Paaswell and Mr. Camille Kamga of the University Transportation Research Center (UTRC) has been instrumental in success of this project.

TABLE OF CONTENTS

LIST OF FIGURES

CHAPTER ONE

STATE OF THE ART ON SMART BRIDGE BEARINGS

1.1 background

Bearings are an integral part of the entire bridge system. Bearings serve to transfer the vertical forces from the bridge superstructure to the pier/abutment, while permitting horizontal in-plane movement of the bridge. While several types of bearings have been used in the past, elastomeric bearings have become increasingly popular because of several advantages when compared with conventional bearings, such as low cost and low maintenance. Elastomeric bearings are fabricated in several configurations ranging from unreinforced elastomeric pads to reinforced bearing systems. Reinforced bearings comprising of layers of elastomer reinforced with alternating layers of steel are used extensively in highway bridge applications because such bearings can be designed in different geometries and heights, and allow for a wide range of in-plane movement while transferring large vertical forces.

Bearings serve to concentrate the force of the entire bridge at a few points. The dynamic response of the bridge is directly dependent upon the stiffness of the bearings. The seismic vulnerability of the bridges is also directly related to the state of the bearings. Measurement of load and shear-strain within bridge bearings can be directly correlated with health and longevity of the structure. Non-operating bearings and tremendous stresses that result are a common factor in bridge failures and are a common maintenance requirement. Therefore, the bearings play a very important role in determining the static, dynamic and the seismic performance of the bridge. Generally, the monitoring of bearings is done through manual visual inspection. This type of inspection is not effective in determining the efficiency of bearings and it doesn't give any information about reaction forces at the different bearings.

The objective of this research is to conduct a feasibility study on the development of sensing technologies (both advanced and conventional) for the cost-effective internal measurement of elastomeric bridge bearing reactions and displacements in real-time. Bridge bearings integrated with such automatic real-time measurement capability are called "Smart Bearings". The real-time measurement of bearing reactions can be used to determine load distribution on supports and piers. A computer model-based performance monitoring can be done by continuously updating the finite element model of the bridge using measured bearing reactions. This updated model will also be useful in forecasting the performance of the bridge during peak traffic loads, seasonal or emergency traffic loading. Bridge reactions obtained through smart bearings can be combined with Bridge Management System (BMS) to optimize maintenance costs of the bridge. Specific benefits of implementing "smart bearings" include a reduction in the maintenance and replacement costs of bridges, and an increase in the safety and reliability of the entire bridge superstructure through continuous automatic monitoring. In essence, smart bearings, by design, will provide the basic information necessary to effectively manage the bridge infrastructure throughout its life cycle. Recently, several advanced sensors have been proposed for applications to structures [Ansari (1997, 1998)[1,2]]. Sensors for use in infrastructure applications, such as Highway Bridge monitoring, have to satisfy very strict criteria that will ensure robustness and long-term performance. In addition, criteria such as ease of implementation, availability of commercial technology, level of expertise required for interpreting the results, low maintenance, etc., play a very important role in identifying an appropriate technology.

The goal of this project has been achieved through three tasks. The main goal of Task I has been to identify appropriate sensors that have potential for bridge bearings applications. This has been achieved through the following subtasks and has been presented in this chapter:

(a) An extensive literature review of behavior of elastomeric bearings and state-of-the-art on the smart bearings.

(b) Objective criteria for selection of sensors.

(c) Information, specifications and reliability of commercially advanced sensors.

The focus of Task II has been to develop possible instrumentation schemes for implementing smart bearings, as presented in Chapter 2. In Task III, costs associated with feasibility of smart bearings have been investigated. This work has been reported in Chapter 3.

1.2 Literature Review on Bearings

1.2.1. Prior Work on Elastomeric bearings

Elastomeric bearings have been used in United States for approximately 40 years and are now used with increasing frequency because of minimal maintenance requirement and low cost. Stanton and Roeder (1982)[3] and Roeder et al (1987, 1989)[4,5] have investigated elastomer material properties, bearing behavior, and failure modes extensively. Their research results largely promote the application of elastomeric bearings. Recommended approaches for the testing of elastomeric bearings are available in Yura et al (2001)[6]. These references[3-6] collectively provide recommended revisions to the design and construction requirements for elastomeric bearings contained in the AASHTO Standard Specifications for Highway bridges (2002)[7].

Elastomer in bridge bearings is either natural rubber or neoprene. Neoprene is a “spring-like” material with a well-defined relationship between the applied force and deformation. Neoprene is a temperature sensitive material, wherein its stiffness increases with decreasing temperature. Both natural rubber and neoprene are complex visco-elastic polymers, and have highly nonlinear, time and temperature dependent stress-strain behavior[4]. Especially, elastomer would be stiffening at low temperature[5]. However, the linear elastic analysis, modified by appropriate empirical factors, appears to provide acceptable accuracy for most bridge bearing applications[3,8,9].

Conventionally, neoprene is the elastomer of choice used in bearings. Neoprene is a “rubber-like” substance which is capable of resisting applied vertical forces while the resistance to in-plane movement, even under the action of a vertical force, is negligible. Neoprene pads when subjected to vertical force, however, exhibit outward bulging. The bulging effect increases as the thickness of the pad is increased. This effect restricts the height of a neoprene pad which can be used effectively for transferring vertical loads. The total in-plane (horizontal) movement allowed by a neoprene pad increases with increase in its thickness. Thus, to obtain a bearing which resists large vertical forces without excessive bulging, while permitting horizontal movement, reinforced elastomeric bearings are used in practice. Typical design of elastomeric bearing for a specific application involves selecting the number of layers of neoprene and the dimensions of the neoprene and steel reinforcing layers.

Elastomeric bearings are made either as unreinforced elastomeric pads or reinforced elastomeric bearings. The elastomer is flexible under shear stress, but stiff against volumetric changes[8, 9]. Under uni-axial compression, the flexible elastomer would shorten significantly and sustain large increases in its plan dimension, but the stiff steel layers restrain this lateral expansion. This restraint induces the bulging and provides a large increase in stiffness under compressive load. As a result, steel reinforced elastomeric bearing are capable of supporting relatively large compressive loads while accommodating large translations and rotations[4]. The stiffness of the bearing controls the loads which the bearing can support and transmit forces. The compressive and rotational stiffness of bearing are approximately proportional to the shape factor[10,11]. Shear stiffness under translational movements is independent of the shape factor.

The first AASHTO specification (1961) for elastomeric bearings addressed only unreinforced elastomeric bearing pads. In 1980, NCHRP 10-20 was established to develop an improved design specification for plain and reinforced elastomeric bridge bearings[3]. Stanton and Roeder (1982)[3] and Roeder et al (1987, 1989)[4,5] did fundamental work on criteria for the bearing design and construction by collecting, evaluating and analyzing the data from a number of laboratory tests. Their work has been adopted by AASHTO consequently. Furthermore, they developed spreadsheets to largely simplify the design of elastomeric bearings[12]. Appendix A contains a brief description of elastomeric bridge bearing design methods.

1.2.2. Prior Work on System of Smart Bearings

The bearings play a significant role in the accommodation of the displacements and development of the forces associated with this movement. Movement at the bearings is part of the proper function of the bridge system. Because the bearing motions are large enough to be captured with commercially available instrumentation, and are indicative of the behavior of the entire bridge system, it is natural to measure those motions to evaluate the bridge system. Such bridge bearings integrated with those automatic real-time measurement capabilities are called "Smart Bearings".

The goal of this research is to conduct a feasibility study on the development of smart bearings. The smart bearings mounted with appropriate sensors would provide data to monitor elastomeric bridge bearing stresses, temperature, bearing strain/strain rate, and bearing lateral displacement. We can use these measured data to determine bearing reactions, dynamic load amplifications, bearing response, and performance of the bridge.

Since the concept of smart bearings is quite recent, little work has been done by researchers in this area. The pioneering study on the development of smart bearing concept using Finite Element Modeling of the entire bridge structure, including the bearings and foundation, was done by Subramaniam (1995)[13], Nims et al (1996)[14], and Nims (2000)[15]. Subramaniam (1995)[13] performed the initial finite element analysis, for an extensive analytical study of the feasibility of using elastomeric bearings for bridge monitoring and condition assessment of a bridge built over Hamilton Avenue in Hamilton County, Ohio. This model considered the effects of moving loads, temperature loads and deterioration on the movement of bearings, and found that shear displacements at bearings due to moving loads are large enough to be detected using appropriate sensors integrated with elastomeric bearings. The displacement of bearings due to temperature effects was found to be considerably higher than that of moving load. The displacements of bearings were shown to change considerably due to deterioration in a direction perpendicular to the spanwise direction. Subramaniam (1995)[13] clearly demonstrated that the deterioration of the bridge superstructure can be easily detected by monitoring the displacements of bearings over a period of time. Although the displacement pattern in the spanwise direction doesn't change, there is a significant shift in the magnitude due to deterioration in the direction parallel to the traffic. Nims (2000)[15] presented the results of investigation and analysis performed on elastomeric bridge bearings. The focus of this research was the measurement of bearing deformations in the field and assessment of the feasibility of using instrumented elastomeric bearings to monitor bridge condition. Innovative aspects of this research are that it focuses on the in-service behavior of bearings by measuring bearing deformations in the field record, and assessing the feasibility of using instrumented elastomeric bearings to monitor bridge condition.

Although the theoretical investigation of Subramaniam (1995)[13], Nims et al (1996)[14] and Nims (2000)[15] on the feasibility of smart bearings is quite extensive and conclusive about its feasibility, there is a need to carry out the development of the sensing technology and its integration with bridge bearings to develop the practical smart bridge bearings. An attempt to develop a smart bridge bearing by integrating it with optical fiber sensors has been presented by Caussignac et al (1996)[16], Schulz et al (1998)[17], Seim et al (1999)[18] and Udd et al (1999)[19]. Caussignac et al (1996)[16] equipped bridge bearings with optical fiber sensor for measuring vertical load. Optical fiber sensors can either be built into the bearing itself or be placed between the girders and bearings. To measure vertical load through the bridge bearing, Caussignac et al (1996)[16] developed a technology based on using fiber optical sensors. The system of three or five fiber optical sensors are incorporated in an external metallic plate and inserted under the bearing.

Schulz et al (1998)[17] are developing a multi-axis strain and temperature sensor based on dual overlaid gratings written onto polarization. The sensor is in the configuration of a load cell with embedded distributed transverse strain sensor, as shown in Figure 1.1[19]. This load cell has the capability to measure transverse strains and strain gradients, and has the potential to measure three axes of strain and temperature simultaneously.

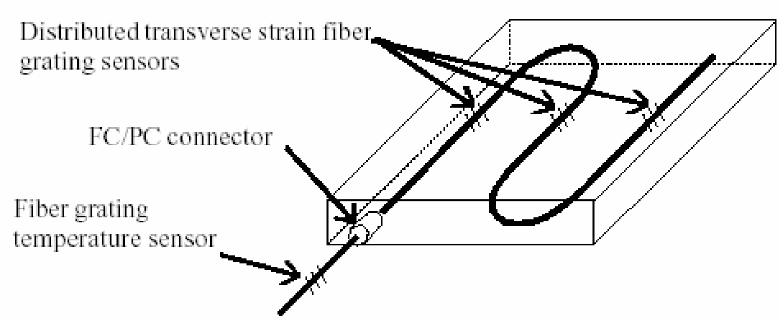

Figure 1.1. Load Cell with Embedded Distributed Transverse Strain Sensing Fiber Grating Sensors

An application of fiber-grating strain sensors is discussed for the historic Horsetail Falls Bridge in the Columbia River Gorge by Seim et al (1999)[18]. This bridge was not designed to carry the traffic loads that are commonplace today. Fiber reinforced plastic (FRP) composite strengthening was selected to increase load carrying capacity of the bridge. Fiber optic grating strain sensors were selected for the long-term monitoring of the bridge, since they potentially have a long service life and can be configured in long gauge lengths.

Research is currently being conducted on embedding single and multi-axis optical fiber strain sensors within liquid molded load cells for bridge bearings by Udd et al (1999)[19]. As seen in Figure 1.2, the "smart bearing" using this sensor is composed of alternating layers of neoprene, steel, and the composite "load cell". The optical fiber strain sensors are embedded into the load cell during fabrication. The measurement of shear-strain and load within bridge bearings can be directly related to the health and longevity of the structure.

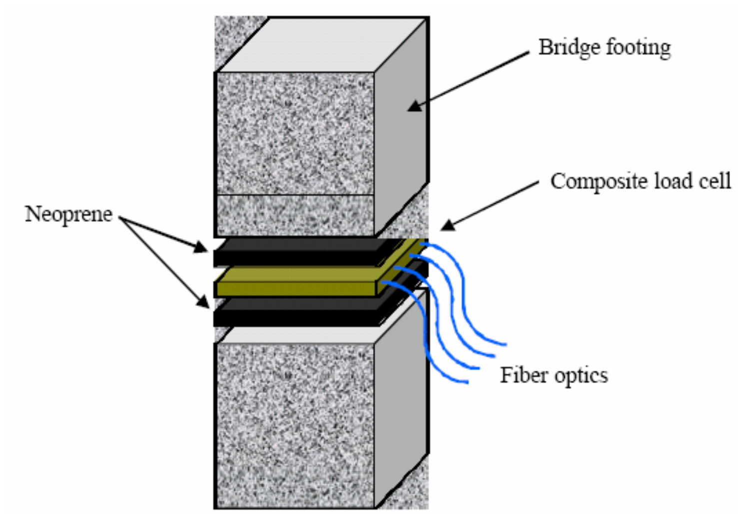

Figure 1.2. Elastomeric Bridge Bearing with Load Cell

However, optical fiber sensors are quite expensive and the cost per bridge bearing may be several times the price of the bearings itself. Consequently, using optical fiber sensors for monitoring of bearings may not be economically feasible. Moreover, optical fiber sensors may require expert maintenance and support to analyze data correctly, and their reliability in harsh field conditions in not well known.

Ghosh et al (2003)[20] have developed a smart inspection unit for overweight truck monitoring problem on the US-Mexico border. This smart unit can identify an overweight vehicle and send the digital picture of vehicles to neighboring inspection station. As shown in Figure 1.3, left side bearings are instrumented with electric resistance strain gages. Through LabVIEW based software, strain and strain-rate history are extracted from bearing sites. The digital camera is controlled through IMAQ Vision. Strain gage values were verified with ANSYS based Finite Element analyses. A Genetic Algorithm based code is developed which takes the “Strain vs Time” and “Strain-rate vs Time” data as input into the program and is able to identify individual vehicles for simple cases. For more complex situation where more number of vehicles are present and moving in different direction, further efforts are underway to use Genetic Algorithm to optimize the number of sensor and their location in the “Smart Inspection System”. The innovative technology is based on the principle that strain and strain-rate history colleted at instrumented bridge bearings can be used to locate the position of the axle, axle-weight, speed and direction of vehicle movement. Results show very clearly that it is possible to determine vehicle characteristics if the bearings are designed and instrumented carefully.

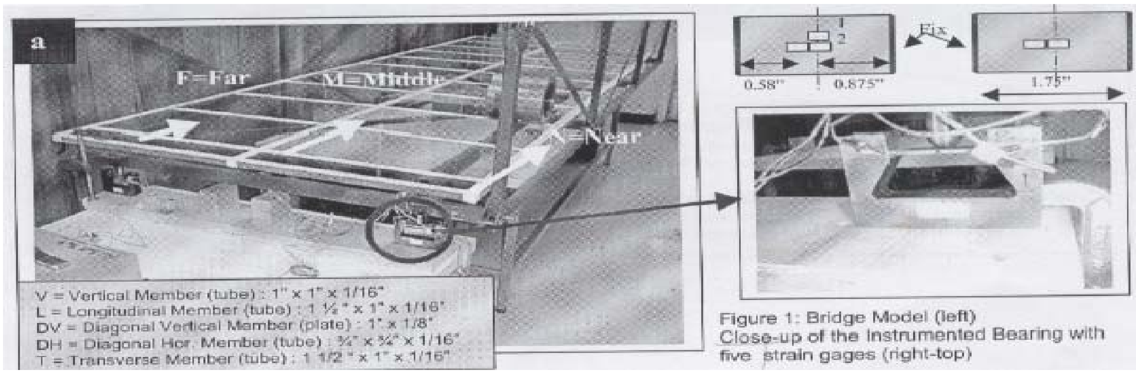

Figure 1.3. Experimental Bridge Bearing Research at University of New Mexico; Bridge Model (left) and Close-up of the Instrumented Bearing with Five Strain Gages (right)

For large stain of more than 10% and localized phenomena, the stain gauges (3000 micro strain range) are not applicable. Recent developments in digital image acquisition techniques, along with the availability of image analysis tools, have provided a method to trace the deformation of flexible continua so that a large strain field can be measured. Lewangamage et al (2004)[21] have developed a modified image analysis algorithms to measure the strain field of bridge bearings. Application of the image analysis algorithms to measure the strain field of rubber shows that it can be used to trace the localized deformation behavior well. Figure 1.4 shows the bearing test set-up in lab. Images of deformation of the specimens were taken using an analog camera and a CCD camera for simple shear tests. Then, through the comparison between the successive acquired images, the displacement of every material point has been obtained. There are four factors that may control the performance of the method: matching criterion, searching strategy, size of the searching window and surface texture condition. The involved matching algorithm is a vital factor. Lewangamage et al (2004)[21] proposed a correlation-based template matching algorithms. However, for the monitoring of the smart bearings onsite, the image analysis method could be a supplementary method only when abnormal large stains can not be measured by regular strain gauges.

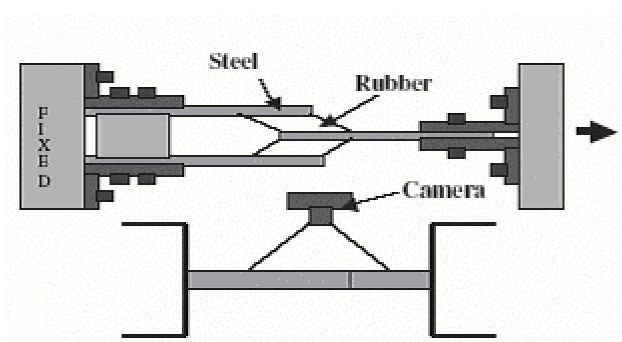

Figure 1.4. Schematic Diagrams of Shear Test Set-ups

Traditionally, large number of discrete sensors such as strain gauges and accelerometers are used in health monitoring of bridge with a vibration-based technique. Alternatively, the structural condition of bridge can be monitored with distributed cable sensor, which can eliminate the reliability and maintenance issue associated with the large quantity of sensors during operation. However, the conventional distributed cable sensor is designed according to the geometric change of cables, which is insensitive to the strain applied on the cable. Chen et al (2004)[22] have developed a novel distributed cable sensor that is significantly more sensitive for measuring strain. For pressure measurements in bridge bearings, it can be designed as flat tape sensor. The idea is to measure a reflection signal when the change in topology of its outer conductor occurs due to pressure effect. The test results show it is sensitive to the change of pressure due to loading. This new cable sensor was designed based on the change in strain conditions instead of the change in geometry of a conventional cable sensor. The two measurement concepts are shown in Figure 1.5.

(a) Cable with geometric change

(b) Cable with topological change

Figure 1.5. Schematic Representations and Model of Coaxial Cable with Loading

1.2.3. Measurement of Bearing Reactions

A known load-deflection behavior of the elastomeric bearings provides a means for direct monitoring of the bridge reactions. The concept of "smart-bearing" can be implemented through careful selection of instrumentation and data collection procedures. Instrumentation of the bridge bearings must satisfy two fundamental requirements:

a. Selection of appropriate variables for measurement which can be relayed into meaningful measures pertaining to the bearing, the bridge and/or the vehicle

b. Selection of appropriate sensors, which allow for obtaining the desired measurements.

a. Selection of variables

To determine the variables to measure from a typical bearing it is important to understand the following:

1. Expected response of an elastomeric bearing to external loads and/or environmental impact: The key aspects of the elastomeric bearing response are summarized below:

   a. Elastomeric bearings behave like vertical springs, which posses a fixed relationship between the applied loading and the measured vertical displacement. Thus, vertical reactions at a bearing can be determined directly from the stresses in the elastomer or indirectly from the measured vertical displacements using the appropriate force-displacement relationship of the bearing. Since the load response of the bearing is temperature dependent, the temperature of the elastomer would have to be measured in addition to the vertical displacement to determine bearing forces indirectly.

b. Elastomeric bearings accommodate large horizontal, in-plane displacements.

c. The elastomeric bearings are known to provide damping to the vertical impact forces and to the vibration of the bridge deck such as those produced by a passing vehicle. Thus, the dynamic response, specifically the acceleration, measured at an elastomeric bearing provides for assessing the dynamic amplification of the vertical load produced by impact.

2. The relationship between the response of the elastomeric bearing and that of the bridge and/or applied loading: Previous research has established that the damage in the deck structure is reflected in the measured reactions at the bearings. Therefore, monitoring bearing reactions provides a means to assess the condition of the bridge.

Based on the previous discussion, the variables of interest are:

i. Stresses in the elastomer
ii. Vertical and horizontal displacements
iii. Vertical acceleration
iv. Temperature of the elastomer

b. Selection of appropriate sensors

Selection of sensors requires a careful consideration of: (a) the expected range of measurement; and (b) the environmental conditions to which a sensor will be exposed to. Various objective criteria for the selection of sensors are described in the next section.

1.2.4. Objective criterion for selection of sensors

Table 1.1 below shows the NYSDOT design requirements for standard type steel laminated elastomeric bearings[23]. Roeder and Stanton (1996) present the following requirements for elastomeric bearings[12]:

- Stress up to 12MPa
- Lateral Displacement <100 mm
- Operating Temperature low to $-35^0 C$
- Compressive load <3500 kN

Table 1.1: NYSDOT Design Requirements for Standard Type Steel Laminated Elastomeric Bearings*

STANDARD TYPE E.L. ELASTOMERIC BEARINGS								
Length (mm)	Width (mm)	Max. Load (kN)	n	h_{rt}	Max. Move. (mm)	Shape Factor	Comp. Area* (sq. mm)	Shear Area* (sq. mm)
150	850	400	2	24	12	4.85	119570	125540
200	850	675	3	36	18	6.20	161770	168040
250	850	1000	4	48	24	7.44	203970	210540

***NYSDOT Bridge Manual, Section 12, Bridge Bearings

Since sensors selected to instrument bridge bearings must be capable of measuring loads and displacements that bearings are subject to, the requirements will be used in developing effective instrumentation scheme to develop smart bridge bearings. The selection of sensors in any instrumentation scheme will depend on the following objective criteria:

- Appropriate measurement range
- Durability to harsh environment
- Instrumentation feasibility
- Financial cost
- Technical expertise required

An extensive literature review has been conducted on various types of sensors satisfying above objective criteria. Appendix B contains a brief description of these sensors.

1.2.5. Bearing measurement goals

(A) Bearing Reactions

- Directly by vertical Stress Measurement;
- By strain and temperature measurement, then through compressive stiffness and strain- stress relationship to obtain stress distribution;
- By displacement and temperature measurement, then through finite element analysis with measured displacement as input or through Δt to get strain and stress using following relations[10].

$$E_c = E\left[1 + f(S^2, v)\right] \tag{1}$$

$$f(S^2, v) = \frac{96v^2}{1-v^2} S^2 \sum_{n=1}^{\infty} \frac{1}{\alpha_n^2 \beta_n^2} \left(1 - \frac{\tanh(\beta_n)}{\beta_n}\right) \tag{2}$$

$$\alpha_n = (n - 1/2)\pi \quad , \quad \beta_n = \left[\alpha_n^2 + 24\frac{1-2v}{1-v} S^2\right]^{1/2} \tag{3}$$

$$p = \frac{E_c A}{t} \Delta t \tag{4}$$

Where E is Young's modulus, v is Poisson's ratio, S is shape factor, and t is the thickness of an internal elastomer layer. Through above steps, the effective compression modulus E_c could be derived. From the measurement of the thickness reduction Δt, p can be estimated[10].

(B) Vehicle characteristics and traffic overloading[20]

- Strain / strain rate history by electric resistance strain gages, then through Genetic Algorithm based code which takes the "Strain vs Time" and "Strain-rate vs Time" data as input into the program and is able to identify the characteristics of each vehicle present on the bridge that contribute to the total strain monitored by the sensor. The individual vehicle effects could be separated.

(C) Impact factors

- Finite element analysis with measured bearing reaction as input.
- Horizontal and vertical acceleration

(D) Performance of bridge

- Displacement and temperature measurement, then through finite element analysis with measured displacement as input

1.2.6. Measurement items and sensors

(A) Strain: strain in bearings can be measured using the following sensors. The measurement ranges of these sensors are listed for convenience.

- Electrical resistance strain gages Range: $\pm 3000\mu\varepsilon$
- Vibrating wire strain gage Range: $\pm 3000\mu\varepsilon$
- Interferometric Fiber Optic Strain Gauges Range: $\pm 5000\mu\varepsilon$
- Digital image acquisition and analysis (Images of deformation of the bearings were taken using an analog camera and a CCD camera)[23]
  Accuracy: $\pm 0.1\varepsilon$

Note: Although there is concern about Vibrating Wire Strain Gauges in dynamic environment, they have been used to instrument highway bridges. Zeroing or drift in case of Electrical Resistance Strain Gauges may be of concern.

(B) Strain Rate: calculated from strain history by subtracting the current strain value from the previous strain value and dividing by the time interval.

(C) Lateral Displacements

- Linear Variable Differential Transformer(LVDT) Range: ± 101 mm
- Fiber optic sensors

(D) Vertical Displacements

- Vertical Gaging LVDT Range: ± 101 mm
- Fiber optic sensors

(E) Acceleration

- Piezo-resistive accelerometer for horizontal and vertical acceleration (The change in the electrical resistance of system is measured and converted into acceleration) Range: $\pm 2g$ to $\pm 100g$

(F) Temperature

- Embedded thermocouple Range: $1800^0 C$ to $-35^\circ C$

(G) Bearing Stress or Vertical Compressive load:

- Optical fiber sensors for vertical load (The shape of the plate grooves, containing the fibers, should be chosen so that the sensor range and offset can be adapted to the operating load.)
- Distributed cable flat tape sensors[22]
- Dynaforce System with Thin-Film Tactile Force Sensing Arrays. These sensing arrays measure force and pressure distribution between mating surfaces making it possible to evaluate the location and magnitude of contact pressure. Range: 0 to 175 MPa

CHAPTER TWO

INSTRUMENTATION SCHEMES FOR SMART BEARINGS

2.1 Instrumentation Objectives

Chapter 1 of the report discussed in details about effective and economic sensing devices for bridge bearing monitoring. The objective of this report is to propose instrumentation schemes to measure bearing reactions. The design of an instrumentation scheme depends on several factors, such as the possible range of movement expected in bridge bearings, typical magnitude reaction forces, and the environmental field conditions experienced by a typical bearing. These factors have been discussed in detail in Chapter 1.

In the design of instrumentation schemes, the following two issues have to be addressed: (a) the data provided by the different sensors mounted on the bearings has to be integrated to provide meaningful information about the loads/ displacements, (b) the instrumentation has to withstand the rigors of the field.

The flow chart in Figure 2.1 presents the concept of data storage and processing. Monitoring data can either be collected continuously for a fixed period of time at regular intervals or the interface can be programmed to store only the daily peak value. Through a programmable interface, the datalogger can be programmed to store daily peak response. In continuous monitoring, data can be stored in the datalogger for certain duration. Processing data can be done in the datalogger itself or data can be retrieved for off-site processing. Behavior of the bearings can be analyzed based on detailed analysis of the continuously measured data. The daily peak values can be used to monitor for extreme events during the monitoring period.

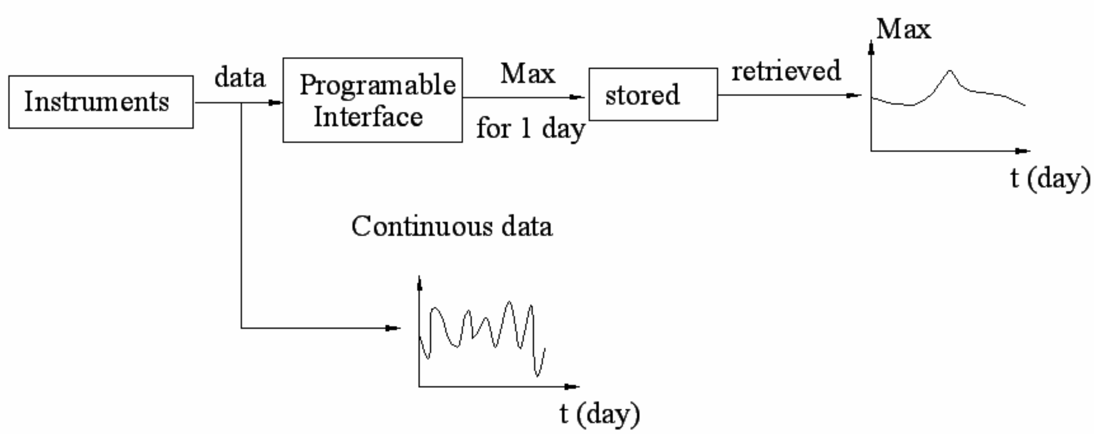

Figure 2.1. Data Storage and Processing Approach

For both continuous and intermittent monitoring, captured data can either be retrieved manually or can be transmitted wirelessly to a remote computer for processing. Wireless transmission can be configured to transmit data automatically or the transmitter can be triggered from a remote computer manually.

2.2 Bearing Monitoring Plan

The following response quantities were identified as being important for effective monitoring of bridge bearings in Chapter 1:

- Bearing Reactions
- Traffic Overloading
- Vertical Acceleration
- Shear Displacements

Instrumentation design for each of the above response quantities are presented in the following subsections.

2.2.1 Instrumentation Design for Bearing Reactions

Bridge bearings are continuously subject to vertical compression, horizontal shear and bending moment. However, the in-service vertical load on bearings is the most important bearing reaction measurement and can be measured using the following approaches:

I. **Reduction in Thickness of Elastomer Layer:** The elastomer used in bridge bearings is a nonlinear visco-elastic material. Further, the vertical load response of an elastomeric bearing exhibits geometric non-linearity. Hence, there is no one-to-one relationship between bearing force and the vertical displacement, and the force-displacement relationship changes with time, temperature, and load history. To avoid the geometric non-linearity in the response of the entire bearing, the approach for estimating the load in the bearing is based on measuring the load in one layer of elastomer. Since the layers of elastomer are in series, the load in each layer is the same. In this approach, reduction in thickness of one elastomer layer, Δt_e, is measured. Then, the vertical bearing reaction force p is calculated using the reduction in elastomer layer, Δt_e, through the following equations,

$$p = \frac{E_c A}{t} \Delta t_e \quad (1)$$

$$E_c = E\left[1 + f(S^2, v)\right] \quad (2)$$

$$f(S^2, v) = \frac{96v^2}{1-v^2} S^2 \sum_{n=1}^{\infty} \frac{1}{\alpha_n^2 \beta_n^2} \left(1 - \frac{\tanh(\beta_n)}{\beta_n}\right) \quad (3)$$

$$\alpha_n = (n - 1/2)\pi\,, \quad \beta_n = \left[\alpha_n^2 + 24 \frac{1-2v}{1-v} S^2\right]^{1/2} \quad (4)$$

where E is the Young's modulus of elasticity, v is Poisson's ratio, S is shape factor, t is the thickness of an internal elastomer layer, and E_c is the effective compression modulus of elastomer layer. The influence of temperature on the material response of the elastomer is accounted for by using the modulus of elasticity as a function of temperature. It is imperative that successful implementation of this scheme requires input of temperature of the elastomer.

Therefore, this approach for determining the vertical force in the bearing requires instrumentation to measure the vertical compression of the elastomer layer and its temperature.

The instrumentation scheme for determining the reduction in thickness of one layer of elastomer involves the use of an LVDT, which is mounted along the central-axis of the bearing as shown in Figure 2.2. To protect the LVDT from the elements, the LVDT shall be placed in a partial depth hole through the bearing. The LVDT shall be attached to the steel plate on the upper surface of the elastomer layer and reacted off of the upper surface of the steel plate at the bottom of the elastomer. The hole shall provide clearance to allow complete range of expected in-plane motion of the bearing. The LVDT will be equipped with a precision ground ball tip to allow free sliding of the steel surface (shown in the inset of Figure 2.2). LVDT assembly shall be covered by flexible rubber sleeve and desiccant. As per discussion of the PI with bearing manufacturer, hole can created in the bearing without

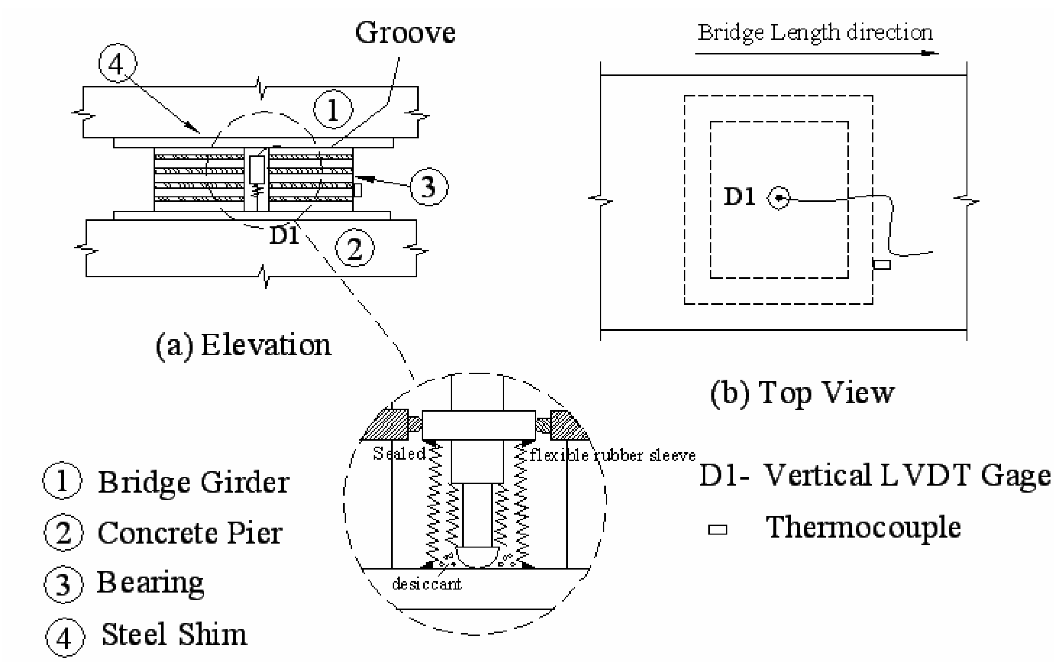

Figure 2.2. Instrumentation for the Measurement of the Reduction the Thickness of Elastomer

It is important to note that the bearing force calculated by Eq.(1) above may be quite different than the actual bearing reaction because of variations in bearing behavior produced by the shear displacement.

Feasibility: *bearing reactions obtained by this approach should only be used as approximate estimate and must be correlated with other measured response quantities.*

II. **Direct measurement of reactions:** Direct bearing force can be measured using the following instrumentation schemes.

(A) Optical Fiber Instrumentation

An instrumentation scheme to measure vertical bearing force using optical fiber sensors is shown in Figure 2.3. In this scheme, an external steel plate incorporated with a system of three or five optical fiber sensors is inserted under the bearing. The measurement of compressive force is based on the microbending technique and light attenuation through optical fibers. To carry out the running threshold of sensors, a V- notch is machined in the steel plate, as shown in Figure 2.3 (c). The shape of the V-shaped notch containing fibers is chosen so that the sensor range and offset can be adapted to the maximum operating load of maximum 1750 psi (12 MPa) pressure. Sensing elements consist of microbended 100/140 multimode fibers through a steel spiral around the polyimide jacket as shown in Figure 2.4. The fiber optic sensor configuration shown in Figure 2.4 is 5-fiber sensor to obtain transverse distribution of bearing reactions (forces). This sensor system provides transverse distribution of forces under the compressive bearing load. Fiber optic sensors embedded in an instrumented plate can be combined with signal acquisition and processing to obtain the time history of the bearing vertical load.

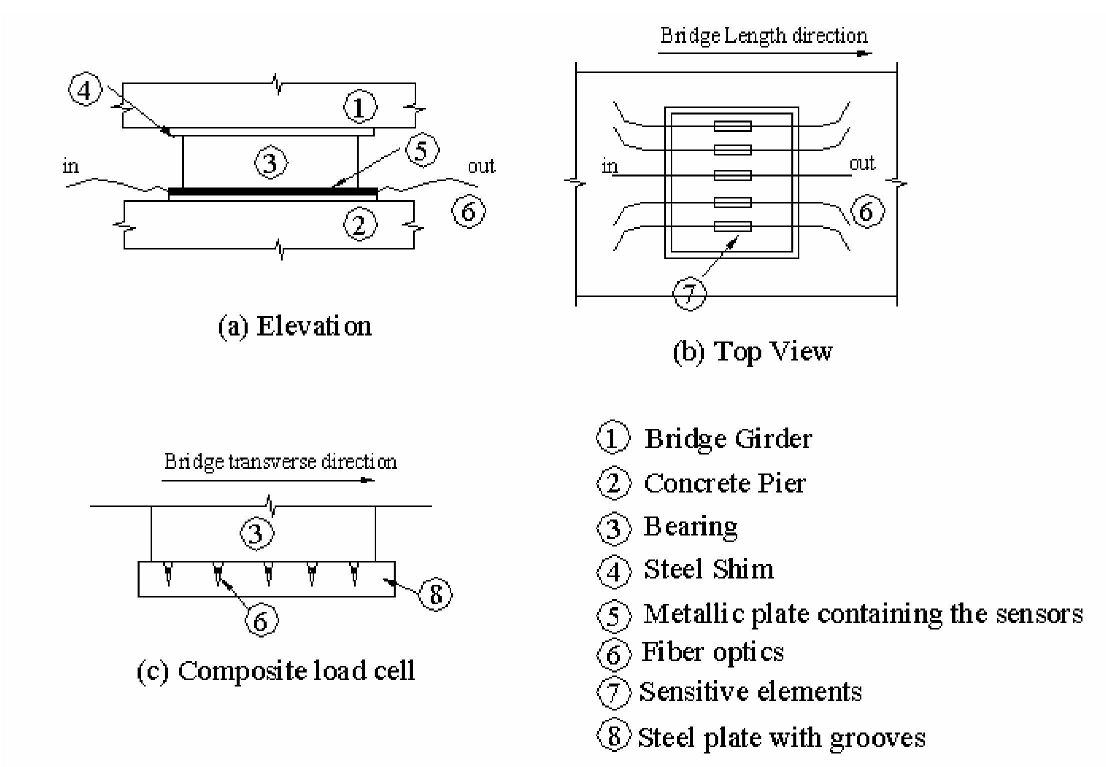

Figure 2.3. Scheme of the Bearing Reaction Force Measuring System

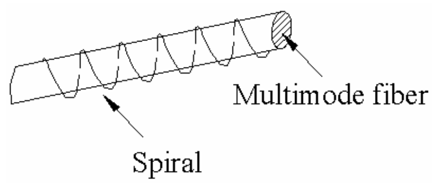

Figure 2.4. Fiber Optic Sensing Element

***Feasibility**: Although optical fiber sensors are commercially available and the technology is well developed, their cost is significantly higher than the actual cost of bearing replacement. This technology has been tested by Caussignac et al (1996)*[16] *for measuring vertical load in a bridge.*

(B) Composite Load Cell with Embedded Multi-Axis Fiber Grating Strain Sensor

Fiber grating strain sensors have several advantages over electrical strain gages, such as greatly reduced size, EMI resistance, and higher temperature capability, making them an ideal choice for smart bearing applications. One such system is a load cell with embedded *multi-axis fiber grating strain sensors*, as shown in Figure 2.5. The multi-axis optical fiber strain sensors are embedded into the load cell during fabrication. This sensor can be incorporated into the bearing by embedding the load cell between alternated layers of neoprene and steel. The embedded fiber-optic sensors have the ability to measure both axial and transverse strains, which are related to pressure strain and shear strain respectively. The ability to embed sensors internally in to the bearing offers several advantages. An internal load cell enables strain sensors to provide more accurate shear and load data compared to surface-mounted sensors. A composite panel with integrated multi-axis fiber grating sensors for the measurement of shear and pressure strains is shown in Figure 2.6. The load cell in Figure 2.6 has been fabricated using a unidirectional carbon fiber by Schulz et al (1998)[17]. The fiber optic sensors were sandwiched in the middle (thickness-wise) of the cell panel shown in Figure 2.6. The total thickness of each panel was about $1/4''$ (7 mm). The maximum shear-sensitivity is obtained by tilting axes of fiber optic sensors at 45 degrees with respect to vertical, and the maximum transverse-strain sensitivity is obtained by orienting sensors axes orthogonal to the plane of the load cell.

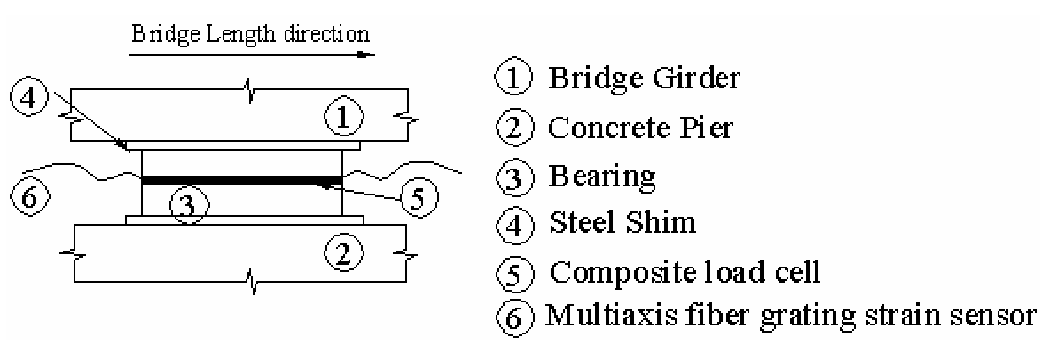

Figure 2.5. Bearing with Integrated Multi-Axis Fiber Grating Strain Sensors

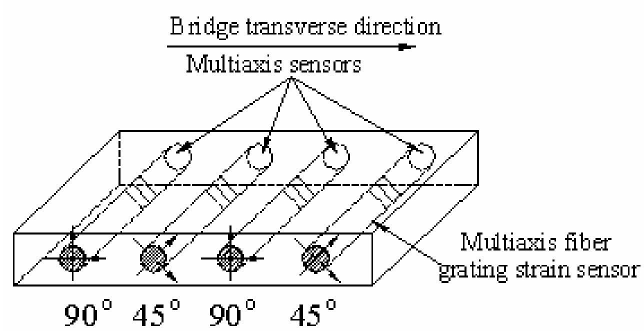

Figure 2.6. Composite Load Cell with Four Embedded Multi-Axis Fiber Grating Strain Sensors

Feasibility: *This sensor has the potential for application of smart bearing. Besides providing information about strain in two directions, the sensors can be embedded inside the bearing. Further, the instrumentation for data acquisition from fiber grating sensors is commercially available. The systems for sensing fiber optic sensors offer the capability of mulit-plexing, which is an advantage for using in multiple bearings. Detailed information on feasibility will be presented in Chapter 3.*

(C) Tactile Pressure Sensor Arrays

Tactile pressure sensors are thin film sensors capable of measuring pressure distribution between the sensor and the contact surface. These sensors have been developed to measure the human skin capabilities in robotics and biomedical engineering applications, and have a high density of distributed sensing elements. These sensing elements are based on different sensor technologies, e.g., piezo-resistive [Beebe et al (1995)[24]], optical [Hok et al (1989)[25]], capacitive [Fearing (1987)[26]], chemical-resistive [DeRossi et al (1989)[27]], inductive [Hackwood et al (1985)[28]], and piezo-electric [Kolesar et al (1992)[29]]. Several of these sensing systems can be adapted in developing plate type sensing elements that can be integrated into bridge bearings. One requirement of these sensors is that they should be capable of withstanding the high pressures applied to bridge bearings. Two such tactile pressure sensors commercially available have the potential for bridge bearings applications.

Dynaforce Tactile Pressure Sensor

The Dynaforce tactile sensor system manufactured by Tekscan, Inc. (www.tekscan.com) consists of two thin, flexible polyester sheets, which have electrically conductive electrodes deposited in varying patterns. In a simplified example shown in Figure 2.7, the inside surface of one sheet forms a row pattern while the inner surface of the other employs a column pattern. The spacing between the rows and columns varies according to sensor application and can be as small as ~0.5 mm (0.0197 inch). Before assembly, thin semi-conductive coating (ink) is applied as an intermediate layer between the electrical contacts (rows and columns). This ink provides the electrical resistance change at each of the intersecting points. When the two polyester sheets are placed on top of each other, a grid pattern is formed, creating a sensing location at each intersection. By measuring the changes in current flow at each intersection point, the applied force distribution pattern can be measured and displayed on the computer screen. Force measurements can be made either statically or dynamically and the information can be seen as graphically informative 2-D or 3-D displays.

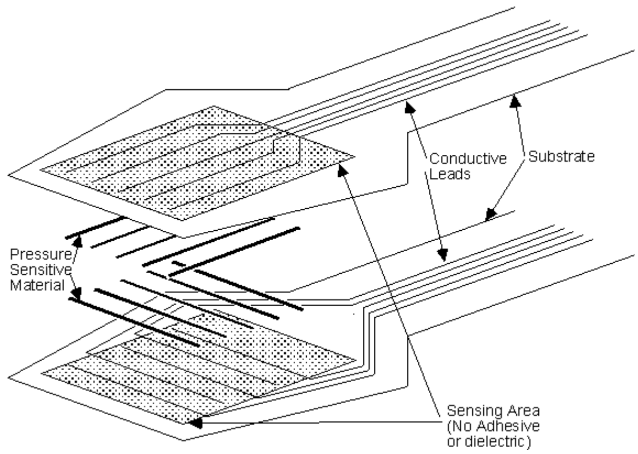

Figure 2.7. Mechanism of Dynaforce Tactile Pressure Sensor

The Dynaforce sensor system is capable of mapping the location and magnitude of contact pressure in the range of 0 to 15,000 psi. The senor system, similar to a paper sheet, can be installed between two steel plates to form a plate sensor. This plate sensor can be installed between bridge bearings and the top plate between the bearing and the girder. Figure 2.8 shows a schematic diagram of the plate sensor and integration of the sensor with bearings.

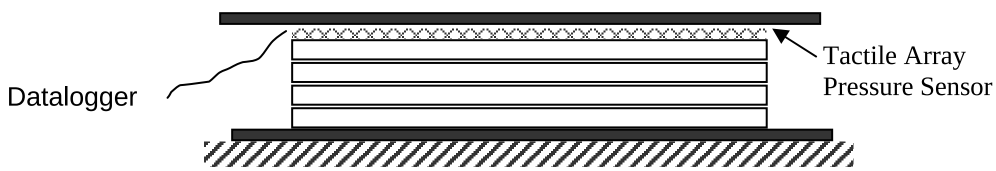

Figure 2.8. Bearing Instrumentation using Tactile Pressure Sensor

One of the major drawbacks of the Dynaforce system is that the datalogger and the software system to capture pressure information are proprietary in nature and the computer system must be on-site. Wireless transmission of data using third party datalogger is currently not possible. Hence, this instrumentation can only be used for intermittent monitoring. Further, these sensors while capable of measuring contact force and pressure over the measuring element, are very sensitive to shear deformation. Hence load sensing application using such elements requires that the in-plane shear deformations are minimized.

Tactarrays Pressure Sensor System

Tactarrays pressure sensor system is similar in principle to Dynaforce tactile sensor system and consists of a Kapton^{TM} membrane system capable of measuring pressure in the range of 0 to 500 psi. Figure 2.9 shows a typical sensor membrane that can be sandwiched between two steel plates similar to that in Figure 2.8. The membrane can be effectively used in the temperature range of –40º to 200º C. One of the advantages of the Tactarrays system is that it can be synchronized with third party dataloggers to transmit pressure data wirelessly. Hence, the system can be used for both continuous and intermittent monitoring without requiring on-site data collection.

Figure 2.9. Tactarrays Pressure Sensor System

Feasibility*: Tactile pressure sensor arrays have tremendous potential for smart bridge bearings and can be used to find reactions as well as pressure distribution. However, these sensors are expensive and may not be economically feasible.*

These sensors, while capable of measuring contact force and pressure over the measuring element, are very sensitive to shear deformation. Hence, applications of these sensors for smart bearings require that in-plane shear deformation be minimized. Therefore, these sensors should be placed between two steel plates, which rest on top of the bearing. These sensors can be incorporated between two steel plates inside the bearing, if no heat is applied at the time of manufacturing.

(D) General Purpose Pressure Sensor Scheme

Several types of pressure transducers are available commercially to measure point pressure between two surfaces. Figure 2.10 shows a commercially available pressure transducer. Such sensors are typically capable of measuring pressure in the range of 0 to 5000 psi with low frequency response at 0.001 Hz. The sensor is suitable for applications in the temperature range of –73 to 135ºC.

The method to obtain bearing reaction using this sensor comprises of monitoring the pressure in the elastomer at four different points. This measurement takes advantage of the fact that the Poisson's ratio of elastomer is close to 0.5 and thus it behaves like fluid when subjected to compression. To measure bridge bearing reactions, four pressures sensor can be installed while the full dead load acts on the bearing, prior to live load application, in the top steel plate of bearing in the configuration shown in Figure 2.11. The pressure sensors are mounted to the sole plate and the diaphragm of the sensor is mounted flush with lower surface of the steel plate such that it presses against the elastomer. If installed while the full dead load acts on the bearing, the sensor would show zero pressure. As additional load is applied to the bearing, the pressure in the bearing would cause the soft elastomer to push against the diaphragm of the pressure sensor. Thus the local pressure in the bearing could be recorded. The uniform pressure on the bearing can be calculated as average measurement of the four sensors or a linear variation in pressure on the bearing can be taken in the longitudinal direction of the bridge, if the pressure reading is not uniform. The total bearing reaction can be calculated by integrating the pressure over the area of the bearing.

Figure 2.10. General Purpose Pressure Sensor

This instrumentation scheme is quite cost effective. For new bearings, threaded holes can be drilled during fabrication of the bearings. For existing bearings, threaded holes must be drilled carefully such that elastomer layer below the sole plate is not damaged. The sensor output can be collected by any commonly available datalogger and transmitted wirelessly for continuous monitoring. Since the sensor is embedded in top bearing plate after bearings have been installed, the sensors are not subject to any static pressure because of bridge weight. Hence, the use of PCB sensors will not be subject any drift of piezoelectric crystal because of static weight of the bridge. Further, the sensor is provided protection from the elements by its location.

This is an innovative idea that has significant potential for success. For installing the transducer internal to the bearing, it can be mounted on any internal steel plate such that the diaphragm is flush with lower surface of that plate. The scheme has significant advantages over load cells that can measure force directly. Load cells with capability to measure bridge reactions are quite big in size. They are usually made of piezoelectric crystals that may undergo drift because of static weight of the bridge over long period of time. The proposed scheme overcomes these disadvantages.

***Feasibility**: Pressure transducers must be installed such that they are not subject to the static pressure due to bridge weight. This can be achieved through construction details at bridge bearings. They can also be installed inside the bearings. This scheme is quite cost effective and has significant potential for success.*

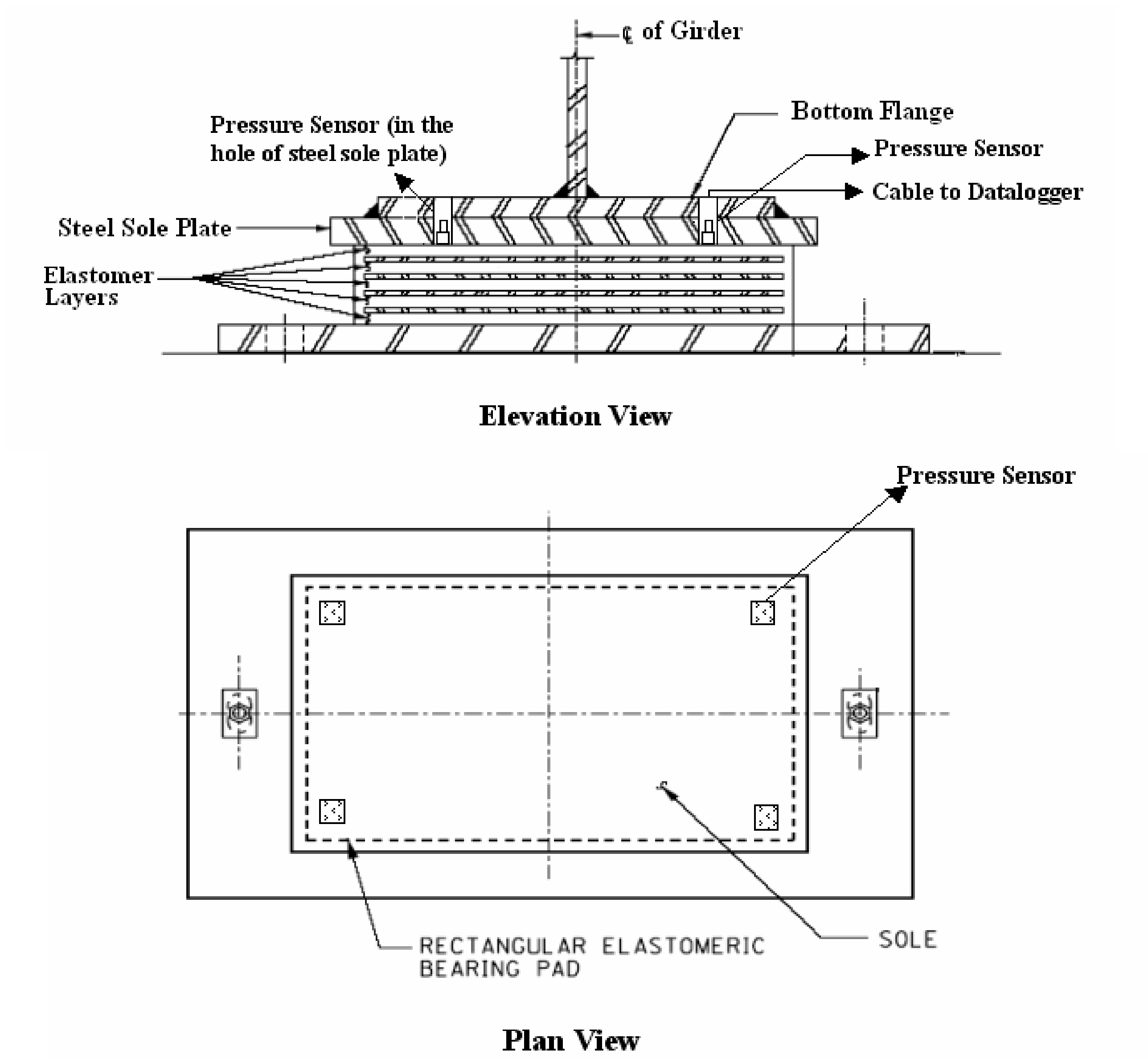

Figure 2.11. Installation of General Purpose Pressure Sensors in Bridge Bearings

2.2.2 Instrumentation Design For Traffic Overloading

As described in Chapter 1, the time history of strain/strain rate collected at an instrumented bridge bearing can be used to determine overweight vehicles. The real time strain can be monitored by electric resistance strain gages. Then, the strain rate can be obtained by differentiating the rate. The bearing strain can be measured by using electrical resistance strain gages**.** Electrical resistance strain gages only need to be installed on the surface of elastomeric bearing, as shown in Figure 2.12. This instrumentation scheme has been used by Ghosh et al (2003)[20] overweight truck monitoring problem on the US-Mexico border. Detailed description of this scheme has been presented in Chapter 1.

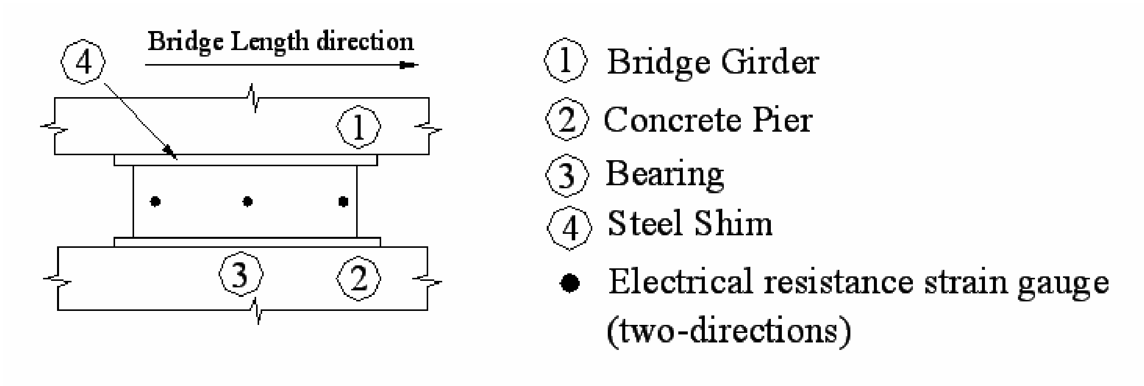

Figure 2.12. Scheme of Strain Gage Setup

Feasibility: *Strain gages offer several advantages such as ease of application, readily available and low-cost data acquisition system etc. However, the bond between the strain gage and the elastomer is achieved using an epoxy, which is often sensitive to water and low temperature. Although this approach has been used by Ghosh et al (2003)* [20] *in a preliminary study to identify overloaded vehicles, the use of strain gages for bridge bearing instrumentation is ultimately infeasible because of reliability and durability concerns.*

2.2.3 Instrumentation Design for Vertical Accelerations

Vertical accelerations are caused because of dynamic characteristics of vehicle-bridge interactions. Detailed information on bridge behavior can be obtained by using measured accelerations as support movement in the finite element dynamic analysis of the bridge. Accelerations can be measured by installing 2 accelerometers as shown in Figure 2.13. Acceleration data can also be used to calculate dynamic amplification factor (or impact factor) through the Finite Element Analysis. Bridges are subject to significant horizontal accelerations only during earthquakes. During traffic loading, vertical vibration of a bridge occurs because of vehicle-bridge interaction. Hence, acceleration measurement in transverse and longitudinal directions is not measured during traffic loading.

Although acceleration measurement will reflect collective effect of unknown speeds, vehicle weights, direction of vehicles, multiple lanes, and multiple loadings, dynamic response of the bridge through FEM model will depend on most dominant dynamic portion of the acceleration data. This portion is contributed by the bridge-vehicle interaction in the vertical direction. Impact factor can be calculated as ratio of displacements at mid-span due to dynamic and static loads. Static load will have to be determined either through bearing reaction measurement (e.g., using pressure transducer). Note that FEM modeling will be required only when dynamic bridge response quantities are desired based on bearing acceleration measurement.

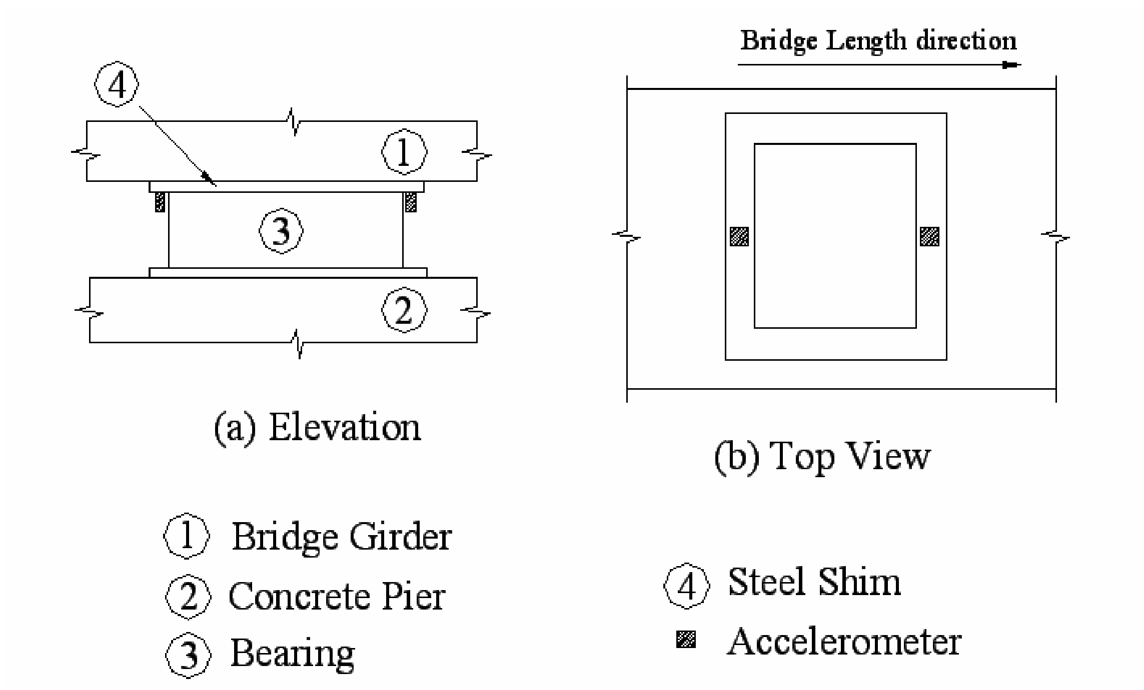

Figure 2.13. Schematic of Accelerometer Setup

2.2.4 Instrumentation Design for Shear Displacement

Temperature change causes thermal movement of the bridge and changes in stiffness of bearings. The shear displacements of the bridge due to temperature are higher than the displacements due to moving load. Changes in vertical displacements are directly dependent on the change in bearing stiffness. The instrumentation design to measure shear movements of bearings is shown in Figure 2.14. Two horizontal LVDT with a range of ± 100 mm can be installed on the bearing to measure shear displacement. LVDT assembly should be protected from environmental exposure by flexible rubber sleeve and desiccant.

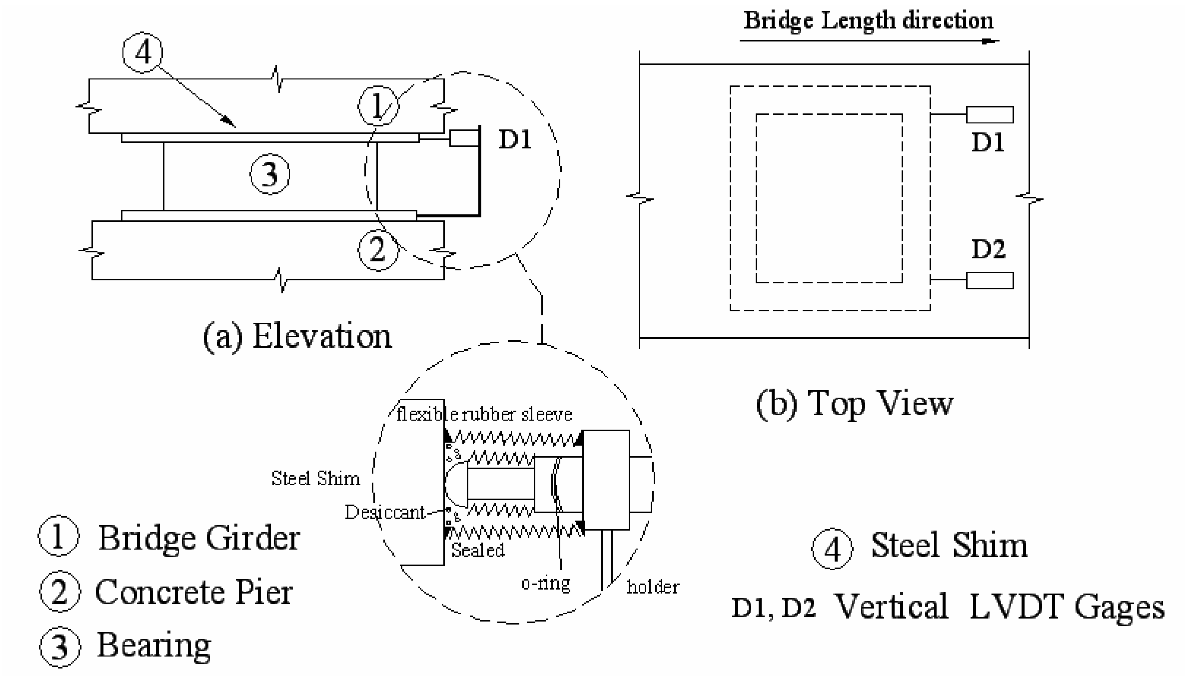

Figure 2.14. Instrumentation Design for Bearing Movements

Using the instrumentation design in Figure 2.14, shear and compression displacements can be calculated as follows. From the measured 2 displacement parameters, rotational movements can also be calculated. The rotational displacement about the vertical axis will be proportional to the difference between displacements Δ_{D1} and Δ_{D1}, measured by LVDTs D1 and D2, respectively. The shear displacement along the bridge can be calculated as

Shear displacement along bridge axis: $\Delta_X = \dfrac{\Delta_{D1} + \Delta_{D2}}{2}$

2.2.5 Comprehensive Instrumentation Schemes

Two comprehensive schemes are proposed for combining information from different sensors to measure the following information:

- Vertical Reactions
- Traffic Overloading
- Dynamic Amplification

- Vertical Acceleration to analyze global behavior of the bridge

Instrumentation Scheme 1

This scheme uses the following sensors for each instrumented bearing:

1. One LVDT
2. Four Pressure Sensors
3. Two Accelerometers
4. One Thermocouple

The information from the LVDT and the thermocouple will be combined to obtain vertical reactions. Vertical reactions can be combined with vertical accelerations in the Finite Element Program to obtain the dynamic load amplifications. The information from the pressure sensors will be used to verify bearing reactions and detect traffic overloading, since recorded peak pressure in bearing elastomers will exceed allowable value (based on bridge rating) during traffic overloading. The proposed instrumentation scheme can be combined with shear displacement scheme in Figure 2.14 if measurement of shear displacement is desired.

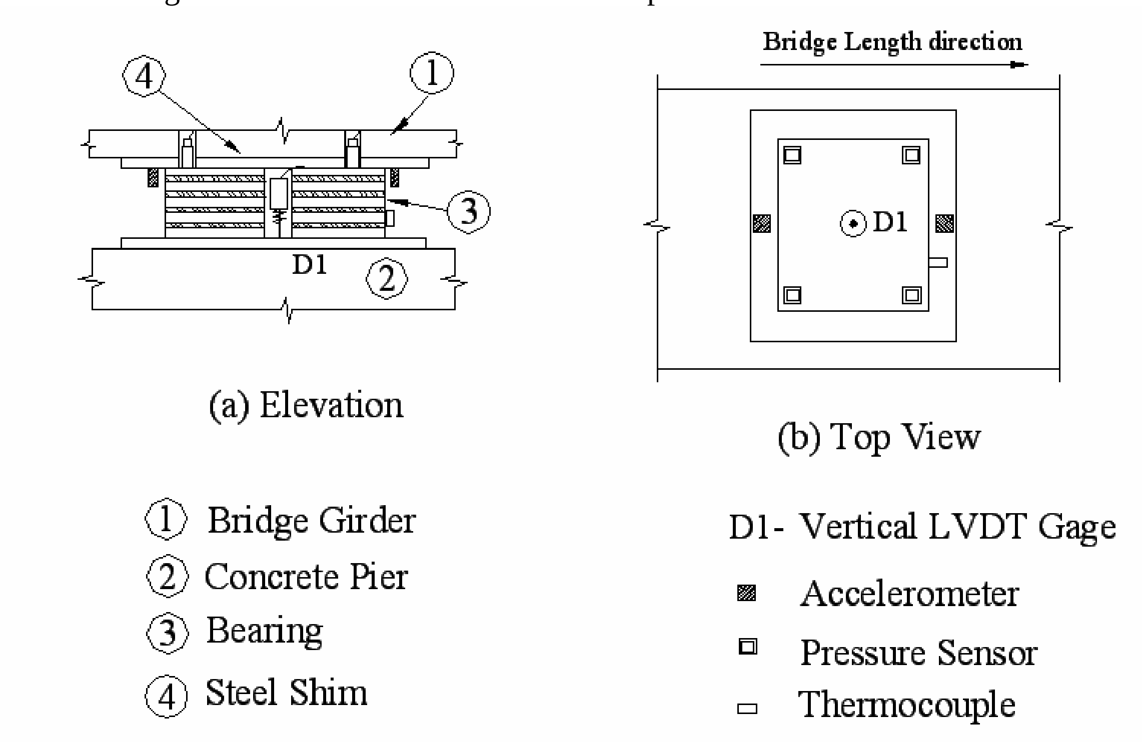

Figure 2.15. Comprehensive Instrumentation Scheme

Instrumentation Scheme 2

The second scheme uses embedded fiber optic sensor scheme in Figure 2.3 to obtain the following:

1. Vertical Reactions
2. Shear Displacement
3. Traffic Overloading

Data from fiber optic sensors in different bearings will be collected in a multiplexed configuration using a single datalogger. The multiplexing will allow probing of different fiber optic sensors using a single light source.

2.3 Data Acquisition System

A data acquisition system collects data from various sensors simultaneously. For the varieties of sensors to be used and wireless data transmission capability desired, CR9000 manufactured by Campbell Scientific meets the requirements of smart bridge bearings. The datalogger has different channel types, e.g., analog (single-ended and differential), pulse counters, switched excitation, continuous analog output, digital I/O, and anti-aliasing filter, to collect measurement from different sensors. It has wide-range of input resolutions, depending of measurement types. Measurement types, recording intervals, and processing algorithms are also programmable. Onboard processing instruction sets contain programmed algorithms that process measurements and output results in the desired units of measurement. The instructions sets also allow for triggered output with pre-trigger data capture capability. Triggers can be based on sensor output, time, and/or user control. The control functions of the dataloggers combined with their programmability gives the capability to call out to phones, pagers, radios, and other devices to report site conditions. Voice-synthesized modems are available, so the system can actually call and alert the user in the event of any abnormal behavior. The datalogger can also be customized for wireless data transmission for both intermittent and continuous monitoring.

The datalogger above can be used for both on-site and wireless data collection. However, any generic data logger can also be used, if wireless transmission and versatile data processing capabilities (alarm list, 2-D Fourier, 3-D Fourier, etc.) are not required. It can support 9 modules, each with 28 single-ended analog inputs (voltage measurements for pressure and displacement) or 14 differential analog inputs (for strain measurement). Hence, a single datalogger can be used to capture data from all instrumented bearings in a bridge.

2.4 Durability and Installation Issues

A datalogger or wireless transmitter will be installed on-site for intermittent or continuous data collection. The data collection system can be installed inside a waterproof data box (similar to electrical switch box). The data box can be locked for security.

The feasibility of integrating instrumentation with the bearing itself has been considered. Complete integration of sensors during manufacturing may not be feasible because of high amount of heat during the bridge manufacturing. The proposed instrumentation scheme 1 can be integrated into the bearing after manufacturing, but before installation. Measurement of shear displacement in this scheme will require the installation of horizontal LVDT after installation of the bearing. The Fiber Optic Sensor scheme in Figure 2.3 can be manufactured off-the-shelf and placed on top of the bearing during the installation of bearing.

Both instrumentation schemes can measures the static weight of the bridges that is experiences by a bearing, if sensors are installed before placing the bearing in the bridge. The number of bearings to be instrumented depends on the objective of instrumentation. If load experienced by each bearing is needed, then all bearings need to be instrumented. On the other hand, one bearing above each row of bents should be instrumented for meaningful data. All collected data can be converted into meaning bridge response quantities using the approach described in this report.

CHAPTER THREE

FEASIBILITY STUDY ON INSTRUMENTED BEARINGS

3.1 Introduction

In Chapter 2 of the project, two instrumentation schemes have been developed for measuring bridge-bearing reactions. The Instrumentation Scheme I in Figure 2.15 consists of the following: (a) One LVDT; (b) four Pressure sensors; (c) two accelerometers; and (d) one thermocouple. In addition, this scheme requires a data logger, which provides for programmable data collection. The LVDT is installed inside the bearing and is protected from the environment. The wire from the LVDT exits the bearing through a groove in the top plate. This will protect the LVDT wire from getting crushed under the bridge weight. Accelerometers are installed outside the bearings and will be protected from environment by installing a cover around it. The Instrumentation Scheme II in Figure 2.3 consists of embedded fiber optic sensors with a data recording system. All fiber-optic sensors are installed between two steel plates (that form a composite load cell) and they are completely protected from the environment. In this Chapter, economic feasibility of the two instrumentation schemes is discussed in detail.

3.2 Instrumentation Costs

For Instrumentation Scheme I, the total cost of instrumentation for one bearing is as follows:

One LVDT:	$409.00
Four Pressure Transducers @ $465 each	$1865.00
Two Accelerometers @ $300 each	$ 600.00
One Thermocouple	$ 30.00
Total Cost for Instrumentation I	$2,904

Assuming 5 girders in a typical span, the estimated cost of instrumentation for a simply supported bridge with 10 bearings is $29,040. Each bearing will require 8 data channels in a datalogger. Hence, a datalogger with typically 80 channels will be needed to capture data from 10 instrumented bearings.

The cost of dataloggers varies depending on the number of channels and data analysis capabilities. Based on price quotations obtained from different vendors, it has been noted that the per-channel cost of datalogger is approximately $250. Hence, a datalogger with 80-channel capability will cost approximately $20,000. This type of datalogger can store data from all the sensors in the built-in hard drive. For applications where it is desirable to transmit data to a base computer, wireless transmission of data can be done by using wireless transmitter manufactured by Campbell Scientific (www.campbellscientific.com) or Microstrain, Inc (www.microstrain.com).

Installation costs of Instrumentation Scheme I will be minimal if the bearing manufacturer integrates these sensors into the bearings. Installation costs will include drilling threaded holes into the bearings for installation of pressure transducer and vertical LVDT.

In situations where bearings under different girders are instrumented, installing permanent cable can be difficult and cost-prohibitive. A much cheaper option can be to use a datalogger with wireless transmission capabilities at each girder. The cost of datalogger with wireless transmission capabilities will be $2,000 to $3,000 higher than conventional datalogger.

The instrumentation scheme II is based on a proprietary fiber optic system developed by Blue Road Research (wwwbluerr.com). This system has previously been tested in highway bridge applications through funding provided by the FHWA. For Instrumentation Scheme II, the cost of the entire fiber optic system includes the sensor units and sensor readout system. The manufactured cost of one sensor unit (consisting of fiber-optic sensors in two directions) is approximately $10,000. The cost of readout unit for measuring strain data from optical fiber source is approximately $38,000. The cost of sensor unit may drop to $5,000 per unit if sensor units are purchased in large numbers.

Although both instrumentation schemes can be integrated in bridge bearings, Instrumentation Scheme I is more economical. However, laboratory testing needs to be carried out before applications of the scheme in actual bridge bearings.

It is noted that the cost of instrumenting 5-girder bridge is approximately $50,000. This cost can be reduced by approximately 20% if transducers are purchased on volume discount to instrument several bridges. For instrumentation of a specific bridge for research purpose, the cost is reasonable.

3.3 Monitoring Costs

Besides instrumentation costs mentioned above, processing of measurement data will add significantly to totals costs. In monitoring of structures, storage of measured data is one of the most challenging issues. In the context of smart bearings, data storage issue can be resolved by programming the datalogger to implement necessary algorithms and filters. This is illustrated in the following.

Since the goal of using pressure transducer and LVDT is to measure peak bearing reactions, datalogger can be programmed to record only peak quantities during every one hour interval. Thermocouple will record the peak temperature during this interval. Acceleration data during this interval will be stored in the temporary buffer and will be replaced by another set of acceleration data if peak pressure and displacement quantities exceed those previously recorded. By following this scheme, less than one Megabytes of total data will need to be stored in the computer for analysis. The cost to program datalogger to perform these tasks will be less than $5,000 and can be used for all bridges to be monitored.

If it is desirable to determine bridge response and impact factor through finite element analysis, measured acceleration data and bearing reaction data can be used. The cost to develop finite element model of the bridge depends on the complexity of bridge modeling, calibration through ambient vibration and load rating. This cost can be minimized by using a bridge for which load rating has already been done by the NYSDOT.

Strain gauges for traffic overloads are not included in Instrumentation Scheme I. If it is desirable, strain gauges can be installed on the bearings. Genetic algorithms are available and can be programmed easily. The genetic algorithms programming can be developed as a standard tool independent of span lengths. Span lengths will be input in the algorithms for detecting traffic overloads.

All dataloggers can be programmed to capture data at different sampling rates. These rates can be customized, depending on bridge characteristics. Overall, the cost of programming the dataloggers to perform monitoring tasks automatically will be approximately $20,000. This part can be used repeatedly for different bridges to be monitored.

3.4 Feasibility Study

For a detailed feasibility study of Instrumentation Scheme I, the PI met Mr. Bob Furchak, the lead civil engineer at AMSCOT Structural Products on October 6, 2005. AMSCOT manufactures various types of bearings used by NYSDOT, including elastomeric bearings. The PI discussed the implementation of the Instrumentation Scheme I with him in detail. According to Mr. Furchak, the hole in the bearing for the installation of LVDT can be created during the manufacturing process by installing a pin of appropriate size and removing the pin after the rubber has been vulcanized. Top plates of appropriate thickness can be predrilled to install pressure sensors. Installation of these sensors will not affect the structural capacity or performance of an instrumented bearing. The suggested modifications to the bearings during the manufacture will only increase the manufacturing cost of a bearing by less than 5% of the cost of the bearing. Hence, the proposed instrumentation Scheme I can be installed in the bearing during its manufacturing process. A standard configuration of datalogger with autonomous data capture and analysis capability can be prepared and used for all instrumented bearings.

REFERENCES

1. Ansari, F. (1997), "Intelligent Civil Engineering Materials, and Structures", ASCE Press, New York, NY, 1997.
2. Ansari, F. (1998), "Fiber Optic Sensors for Construction Materials and Bridges", Technomic Publishing Co., Lancaster, PA, 1998.
3. Stanton, J. F. and Roeder, C. W. (1982), "Elastomeric Bearings--Design, Construction, and Materials", National Cooperative Highway Research Program Report 248, Transportation Research Board, 1982.
4. Roeder, C. W., Stanton, J. F. and Taylor, A.W. (1987), "Performance of Elastomeric Bearings", National Cooperative Highway Research Program Report 298, Transportation Research Board, 1987.
5. Roeder, C. W., Stanton, J. F. and Feller T. (1989), "Low Temperature Behavior and Acceptance Criteria for Elastomeric Bridge Bearings", National Cooperative Highway Research Program Report 325, Transportation Research Board, 1989.
6. Yura, M. J., Kumar, A., Yakut, A., Topkaya, C., Becker, E., and Collingwood, J. (2001), "Elastomeric Bridge Bearings: Recommended Test Methods", National Cooperative Highway Research Program Report 449, Transportation Research Board, 2001.
7. Standard Specifications for Highway Bridges (2002), American Association of State Highway and Transportation officials (AASHTO), 17th Edition, Washington, D.C., 2002.
8. Roeder, C. W. and Stanton, J. F. (1983), "Elastomeric Bearings: State-of-the Art", the Journal of Structural Engineering, Vol. 109, No.12, December 1983, pp. 2853-2871.
9. Roeder, C. W. and Stanton, J. F. (1991), "State-of-the-Art Elastomeric Bridge Bearing Design", ACI Structural Journal, Vol. 88, No.1, Jan-Feb 1991, pp. 31-41.
10. Koh, C. G. and Kelly, J. M. (1989), "Compression Stiffness of Bonded Square Layers of Nearly Incompressible Material", the Journal of Structural Engineering, Vol. 11, No.12, January 1989.
11. Gent, A. N. and Lindley, P. B. (1959), "The Compression of Bonded Rubber Blocks", 1959. Proc. Inst. Mech. Eng, 173(3), 111-117.
12. Roeder, C. W. and Stanton, J. F. (1996), "Steel Bridge Bearing Selection and Design Guide", Vol. II, Chap. 4, Highway structures Design Handbook, American Iron and Steel Institute, 1996.
13. Subramaniam, K. V. (1995), "Feasibility of Using Instrumented Elastomeric Bearings for Bridge Monitoring and Condition Assessment," M.S. Thesis, University of Toledo, 1995
14. Nims, D. K., Subramaniam, K., Parvin, A. and Aktan, A. E. (1996), "The Potential for the Use of Elastomeric Bearings in an Intelligent Bridge System", Transportation Research Board 75th Annual Meeting, Washington, DC, January 1996
15. Nims, D. K. (2000), "Instrumented Elastomeric Bridge Bearings", ODOT Project No. 14647(0), Final Report, University of Toledo January 2000
16. Caussignac, J.-M., Barbachi, M. and Chabert, A. (1996), "Bridge Bearings Equipped with Optical Sensor for Monitoring Vertical Load Through the Support", Proceedings of the SPIE, Vol. 2719, pp. 220-228.

17. Schulz, W. L., Udd, E., Seim, J. M. and McGill, G. E. (1998), “Advanced Fiber-Grating Strain Sensor Systems for Bridges, Structures, and Highways”, SPIE Proceedings, Vol. 3325, p. 212.
18. Seim, J., Udd, E., Schulz, W. L., Morrell, M., Laylor, H. M. (1999), “Health Monitoring of an Oregon Historical Bridge with Fiber Grating Strain Sensors", SPIE Smart Structures and Materials Symposium, Newport Beach, CA. March, 1999.
19. Udd, E., Schulz, W. L., Seim, J., Corona-Bittick, K., Dorr, J., Slattery, K. T., Laylor, H. M., McGill, G. E., Chase, S. B. (1999), “Fiber Optic Smart Bearing Load Structure”, SPIE Nondestructive Evaluation Techniques for Aging Infrastructure, & Manufacturing Symposium, Newport Beach, CA. March, 1999.
20. Ghosh, A. K., Maji, A., and Dasgupta, D. (2003), “Smart Inspection Unit for NAFTA Trucking Problem”, University of New Mexico, Tech Report to the New Mexico State Highway and Transportation Department, June, 2003.
21. Lewangamage, C. S., Abe, M., Fujino, Y. and Yoshida, J. (2004), “Strain Field Measurements of Rubber by Image Analysis and Design Criteria for Laminated Rubber Bearings”, Earthquake Engineering and Structural Dynamics 2004; 33: P445–464
22. Chen, G., Mu, H., Pommerenke, D., and Drewniak, J. L. (2004), “Damage Detection of Reinforced Concrete Beams with Novel Distributed Crack/Strain Sensors”, accepted for publication in the International Journal of Structural Health Monitoring (2004).
23. NYSDOT Bridge Manual (2002), New York State Department of Transportation, 3rd Edition, April 2002.
24. Beebe, D.J., Hsieh, A.S., Denton, D.D. and Radwin, R.G. (1995), “A silicon force sensor for robotic manipulation”, *Proc. of the 7th Int. Conf. on Advanced Robotics,* 1995, pp. 889–894.
25. Hok, B., Tenerz, L. and Gustafson, K. (1989), “Fiber-optic sensors: A micro-mechanical approach”, Sensors and Actuators 17 (1989), 157–166.
26. Fearing, R.S. (1987), “Some experiments with tactile sensing during grasping”, Proc. of the IEEE Int. Conf. On Robotics and Automation, 1987, pp. 1637–1643.
27. DeRossi, D., Lazzeri, L. and Domenici, C., Nannini, A. and Basser, P. (1989), “Tactile sensing by an electromechano-chemical skin”, Sensors and Actuators 17 (1989), 107–111.
28. Hackwood, S., Beni, G., Hornak, L.A., Wolfe, R. and Neson, T.J. (1985), “A torque-sensitive tactile sensor array for robotics”, Int. J. Robotics Res. 2 (1985), 46–50.
29. Kolesar, Jr., E.S., Reston, R.R., Ford, D.G. and Fitch, Jr., R.C. (1992), “Multiplexed piezoelectric polymer tactile sensor”, J. Robotic System 9 (1992), 37–63.
30. AASHTO LRFD Bridge design Specifications (1998), second edition.
31. Roeder, C. W., Stanton, J. F., and Feller, T. (1990), “Low Temperature Performance of Elastomeric Bearings”, the Journal of Cold Regions Engineering, Vol.4, No.3, September 1990. ASCE.
32. Doody, E. and Noonan, J. E. (1998), “Long-Term performance of Elastomeric Bridge Bearings”, Special Report 129, Transportation Research and Development Bureau, New York State Department of Transportation (NYSDOT), March 1998.

APPENDIX A

DESIGN AND REVIEW OF ELASTOMERIC BRIDGE BEARINGS REINFORCED WITH STEEL

A-1. Summary

Elastomeric bearings have been used in United States for approximately 40 years and now are used with increasing frequency because of their minimal requirement of maintenance and low cost. Steel reinforced elastomeric bearings have uniformly spaced layers of steel and elastomer. The elastomer is flexible under shear stress, but stiff against volumetric changes[8,9]. Under uni-axial compression, the flexible elastomer shortens significantly and sustains large increase in its plan dimension, but the stiff steel layers restrain this lateral expansion. This restraint by the steel layer induces bulging and causes a large increase in stiffness under compressive load. This permits a steel reinforced elastomeric bearing to support relatively large compressive loads while accommodating large translations and rotations[4].

The first AASHTO specification (1961) for elastomeric bearings addressed only unreinforced elastomeric bearing pads. In 1980, NCHRP project 10-20 was established to develop an improved design specification for plain and reinforced elastomeric bridge bearings[3]. Roeder and Stanton (1982)[3] developed guidelines for bridge bearings by collecting, evaluating and analyzing a lot of data. The proposed inspection has been adopted by AASHTO consequently. Furthermore, they made a spreadsheet to largely simplify the design work[12].

A-2. Bearing Capabilities for Steel Reinforced Elastomeric Bearing

As per AASHTO LFRD Bridge Design Specifications, main design parameters for bridge bearings are: (i) applied loads (ii) translations, and (iii) rotations. Design loads are mainly reactions of the bridge superstructure. Movement (translations & rotations) is caused by bridge skew and curvature, initial condition, settlement of supports, and thermal effects[3].

There are many bearing types, such as elastomeric pads, steel reinforced elastomeric bearings, pot bearing, PTFE, roller bearings, etc. Table A-1 below shows load and movement capacities of various types of bridge bearings[12]. It is observed from Table A-1 that the range of capacities for elastomeric bearings is:

- 225 kN < Service Load < 3500 kN
- 0 mm< Translation <100mm
- Rotation <0.04 rad

Elastomeric bearings should be used if the range of forces and movements satisfies the requirement of above elastomeric bearings. Otherwise, other types of bearings should be used.

Table A-1 Summary of Bearing Capabilities

Bearing Type	Load (kN)		Translation (mm)		Rotation (Rad.)	Costs	
	Min.	Max.	Min.	Max.	Limit	Initial	Maintenance
Elastomeric Pads							
Plain (PEP)	0	450	0	15	0.01	Low	Low
Cotton Duck (CDP)	0	1400	0	5	0.003	Low	Low
Fiberglass (FGP)	0	600	0	25	0.015	Low	Low
Steel Reinforced Elastomeric Bearing	225	3500	0	100	0.04	Low	Low
Flat PTEE Slider	0	>10000	25	>100	0	Low	Moderate
Pot Bearing	1200	10000	0	0	0.02	Moderate	High

A-3. Design of Steel Reinforced Elastomeric Bearing by Using Spreadsheet (1998 AASHTO LRFD Specifications[30] and 1996 Design Guide[12])

A-3.1. *Input Data for Design Spreadsheet*

Following input data are required for the spreadsheet based design of elastomeric bearings.

- **Minimum and maximum shear modulus *G***
  - ✧ If only the hardness of the elastomer is known, input the corresponding shear modulus range based on Table A-2 below as minimum and maximum shear modulus[30,7].
  - ✧ If the chosen elastomer is defined by shear modulus, enter the same value as minimum and maximum shear modulus.
  - ✧ For steel reinforced elastomeric bearings, the shear modulus values are always in the range of 0.55 to 1.25 MPa .

Table A-2: Elastomer Properties at Different Hardness

Hardness	50	55	60
Shear Modulus (Psi) at 73^0F (MPa)	95-130 0.68-0.93	113-165 0.81-1.18	130-200 0.93-1.43
$\bar{k}$	0.75	0.675	0.6

- $\bar{k}$
  - ✧ As a constant of elastomer material property, $\bar{k}$ only depends on hardness (see Table A-2 above)

- **Yield strength of the steel plate** F_y

- The bearing manufacturers only use AASHTO M270 Grade 250 as steel plates with $F_y = 250\text{MPa}$, (36 Ksi) in bearings[12].

- **Fatigue limit stress of steel** $(\Delta F)_{TH}$
  - For steel reinforcement layers without holes or discontinuities, $(\Delta F)_{TH} = 165\text{MPa}$, (24 Ksi)[12].

- **Thickness of elastomeric cover (top + bottom) layer (** h_{cover} **)**
  - Steel-reinforced elastomeric bearings shall consist of alternate layers of steel reinforcement and elastomer bonded together. In addition to any internal reinforcement, bearings may have external steel load plates bonded to either top or bottom, or both top and bottom elastomer layers. Typically, h_{cover} =3mm.

- **Service load (dead load** P_{DL}**, live load** P_{LL}**)**
  - Live load means truck loading.

- **Rotation of girder at bearing** θ_{TL}
  - Normally, the given value is for the rotation axis in transverse direction.

- **Shear displacement of bearing** Δ_s
  - Δ_s should be taken as the extreme displacement caused by shrinkage, creep, and post-tensioning, combined with thermal effects computed in accordance with Article 3.12.2 of the AASHTO Specification[30].

- **Translation fixed condition in *x*, *y* direction**
  - The *x* direction is assumed along the longitudinal axis of the bridge. The *y* direction is assumed along the transverse axis of the bridge.
  - The translation is always zero in the *x* direction, since the bridge is not considered to stretch in longitudinal direction. If the bearing is not free to sway in transverse direction, the translation in the *y* direction is also zero.

Note: The consistent unit system of either (MPa, mm, kN) or (Ksi, in, Kip) is used in the spreadsheet.

A-3.2. *Output Data for Design Spreadsheet*

The output of design results are as following:

- **Bearing dimension along the transverse axis of the bridge *W***
  - W should be as large as practical to permit rotation about the transverse axis and to stabilize the girder during erection. Usually, W= width of bottom flange of the girder – 25 mm (or 1 in).

- **Bearing dimension along the longitudinal axis of the bridge *L***

- ✧ Usually, $W > L$.

- **Thickness of the single internal elastomer layer h_{ri}, not including the thickness of steel plate**
  - ✧ Typically, elastomer layers have a thickness range of 6 to 15 mm. All internal layers of elastomer shall be of the same thickness, because the thickest layer controls the strength and stiffness of the bearing resisting compressive load[30].

- **The Number of internal elastomer layers *N*. (the number of steel plate is *N+1*)**
  - ✧ There are four bounds for the number of internal elastomer layers in design. Among them, three lower bounds are due to shear deformation, compressive stress under combined compression and rotation, and minimum load to prevent uplift; one upper bound is due to stability.

- **Thickness of one layer of steel reinforcement h_s**
  - ✧ 2 mm or 3 mm thickness is achievable by most bearing manufacturers.

Note: The design of a steel reinforced elastomeric bearing requires an appropriate balance of compressive, shear and rotational stiffnesses.

A-4. Design Steel Reinforced Elastomeric Bearing by Hand Calculation (1998 AASHTO LRFD Specifications[30] and 1996 Design Guide[12])

Two design procedures for elastomeric bearings are provided in the AASHTO LRFD specification. Bearings reinforced with steel may be designed either by the Method A or Method B[12,30,7,5]. The step of Method B discussed below is programmed in spreadsheet approach discussed previously.

Using either method, design should consider the control of the stress in the steel reinforcement and the strain in the elastomer. This is done by controlling the elastomer layer thickness and shape factor of the bearing. Fatigue, stability, delamination, yield and rupture of the steel reinforcement, stiffness of the elastomer, and geometric constraints must all be satisfied.

The stress limits associated with Method A usually result in a bearing with a lower capacity than a bearing designed using method B. This increased capacity resulting from the use of Method B requires additional testing and quality control[12,30,7,5]. Method B makes more refined designs possible at the expense of increased design effort. Hence, Method B should only be used by experienced engineers and researchers.

Step-by–step summaries of these two methods are presented in the following.

A-4.1. *Method A*

Method A is quick, simple, and safe for a wide range of applications.

- **Minimum Elastomer Thickness for Shear Δ_s**

$$h_{rt} \geq 2\Delta_s \tag{A-1}$$

h_{rt} = Total elastomer thickness in an elastomeric bearing;

Δs = Shear displacement of bearing, which is one of the prerequisite data for design. Δ_s is caused by shrinkage, creep, and post-tensioning, combined with thermal effects computed in accordance with Article 3.12.2 of the AASHTO Specification[30].

- **Minimum Dimensions for Stability**

$$h_{rt} \le L/3,\ W/3, \text{or } D/4 \qquad \text{(A-2)}$$

L and W are bearing dimensions along the longitudinal and transverse axis of the bridge, respectively, and *D* = diameter of round elastomer pad.

Hence, for rectangular bearings, conditions on dimensions are

$$W \ge L \ge 3\mathrm{h}_{\mathrm{rt}} \qquad \text{(A-3)}$$

- **Minimum Area for Load**

$$\sigma_{C,TL} \le 6.895\,\mathrm{MPa} \qquad \text{(A-4)}$$

where $\sigma_{C,TL}$ = the average compressive stress under total load (dead load plus live load) $= P_{DL+LL} / A$. Hence,

$$A \ge P_{LL+DL} /(6.895\,\mathrm{MPa}) \qquad \text{(A-5)}$$

$A = L \times W$. Hence, preliminary values of *L* and *W* can be estimated with both (A-3) and (A-5).

Since $\sigma_{C,TL} \le GS$,

$$S \ge \sigma_{C,TL} / G \qquad \text{(A-6)}$$

where *S* = shape factor. The minimum shear modulus, *G*, is taken as the least favorable value.

Since $S = \dfrac{A}{2h_{ri}(L+W)}$, the thickness of a single internal elastomer layer can be obtained as

$$h_{ri} \le \frac{A}{2S(L+W)} \qquad \text{(A-7)}$$

Typically, elastomer layer have a thickness range of 6 to 15 mm. The cover (top and bottom) layer, h_{cover}, is 1/8" (3mm).

$$h_{rt} = Nh_{ri} + 2h_{cover} \qquad \text{(A-8)}$$

N is the number of internal elastomer layers.

- **Rotation Requirement**

Rectangular bearings should satisfy the following conditions:

$$\begin{cases} \sigma_{C,TL} \ge 0.5GS(\dfrac{L}{h_{rt}})^2 \theta_{TL,x} \\ \sigma_{C,TL} \ge 0.5GS(\dfrac{W}{h_{rt}})^2 \theta_{TL,Z} \end{cases} \qquad \text{(A-9)}$$

Otherwise, some adjustments are needed for previously estimated values.

In Eq.(A-9), $\theta_{TL,x}$ and $\theta_{TL,Z}$ are the service rotation due to total load about the transverse and longitudinal axes, respectively.

In Eq.(A-9), the maximum value of shear modulus, *G*, is used as the least favorable value. The number of internal elastomer layers, *N*, can be estimated with both (A-8) and (A-9).

- **Minimum Reinforcement Thickness**

The thickness of the reinforcement, h_s, shall satisfy the following conditions:

at the service limit state: $$h_s \geq 3h_{ri}\sigma_{C,TL} / F_y \qquad \text{(A-10)}$$

at the fatigue limit state: $$h_s \geq 2h_{ri}\sigma_{C,LL} / (\Delta F)_{TH} \qquad \text{(A-11)}$$

where $(\Delta F)_{TH}$ = Fatigue limit stress of steel =165 MPa, or 24 Ksi for steel reinforcement layers without holes or discontinuities.

For fabrication, 2 mm ($1/16''$) is the minimum thickness for laminates.

Based on steps above, the design shear force is obtained as

$$H = \frac{GA\Delta_s}{h_{rt}} \qquad \text{(A-12)}$$

G here uses the maximum shear modulus.

Hence, the total thickness of bearing is obtained as

$$t_{total} = Nh_{ri} + 2h_{cover} + (N+1)h_s = h_{rt} + 2h_{cover} + (N+1)h_s \qquad \text{(A-13)}$$

A-4.2. *Method B*

The design Method B results in higher compressive stresses and more slender bearings. As a result, the substructure is subject to smaller horizontal forces. To qualify for the more liberal design, the bearings should be subjected to more rigorous tests.

- **Design for the Compressive Stress**

For bearings subject to shear deformation:

$$\sigma_{C,TL} \leq 1.66GS \leq 11\,\text{MPa}, \; \sigma_{C,ll} \leq 0.66GS \qquad \text{(A-14)}$$

For bearings fixed against shear deformation:

$$\sigma_{C,TL} \leq 2.00GS \leq 12\,\text{MPa}, \; \sigma_{C,ll} \leq 1.0GS \qquad \text{(A-15)}$$

where $\sigma_{C,TL}$ = the average compressive stress under total load (dead load plus live load) $= P_{DL+LL} / A$; and $\sigma_{C,ll}$ = the average compressive stress under live load.

For example, when designing a bearing subject to shear deformation:

$$A \geq P_{LL+DL} / (11\,\text{MPa}) \qquad \text{(A-16)}$$

We can choose preliminary values of *L* and *W* based on this condition.

Additionally, $$S \geq \sigma_{C,TL} / 1.66G \qquad \text{(A-17)}$$

where *G* is the minimum shear modulus as the least favorable value.

Since $S = \dfrac{A}{2h_{ri}(L+W)}$, the thickness of a single internal elastomer layer can be obtained as

$$h_{ri} \leq \frac{A}{2S(L+W)} \qquad \text{(A-18)}$$

Typically, elastomer layers have a thickness range of 6 to 15 mm. From (A-18), we can try a value for h_{ri}, and get S. Then, check for live load as

$$\sigma_{C,LL} = P_{LL} / A \leq 0.66GS \qquad \text{(A-19)}$$

- Minimum Thickness for Shear Δ_s

$$h_{rt} \geq 2\Delta_s \qquad \text{(A-20)}$$

h_{rt} and Δs are defined previously in A-4.1.

$$h_{rt} = Nh_{ri} + 2h_{cover} \qquad \text{(A-21)}$$

The cover (top + bottom) layer, h_{cover}, is 1/8" (3mm). We can try a value of the number of internal elastomer layers, N, based on this criteria.

- **Combined Compressions and Rotation Requirements**

Bearings shall be designed so that uplift does not occur under any combination of loads and corresponding rotations.
Rectangular bearings may be taken to satisfy uplift requirements if they satisfy:

$$\sigma_{C,TL} > 1.0GS(\frac{\theta_{TL}}{N})(\frac{B}{h_{ri}})^2 \qquad \text{(A-22)}$$

Rectangular bearings subjected to shear deformation shall also satisfy:

$$\sigma_{C,TL} < 1.875GS\left\{1 - 0.200(\frac{\theta_{TL}}{N})(\frac{B}{h_{ri}})^2\right\} \qquad \text{(A-23)}$$

Rectangular bearings fixed against shear deformation shall also satisfy:

$$\sigma_{C,TL} < 2.25GS\left\{1 - 0.167(\frac{\theta_{TL}}{N})(\frac{B}{h_{ri}})^2\right\} \qquad \text{(A-24)}$$

where N is the Number of internal elastomer layers. In above equations, the maximum value of shear modulus, G, is used as the least favorable value. B is the horizontal plan dimension normal to the axis of rotation.

- **Stability Requirement**

If the bridge deck is free to translate horizontally

$$\sigma_{C,TL} \leq G / \left\{\frac{3.84(h_{rt} / L)}{S\sqrt{1 + 2L / W}} - \frac{2.67}{S(S+2)(1 + L / 4W)}\right\} \qquad \text{(A-25)}$$

Otherwise

$$\sigma_{C,TL} \leq G / \left\{\frac{1.92(h_{rt} / L)}{S\sqrt{1 + 2L / W}} - \frac{2.67}{S(S+2)(1 + L / 4W)}\right\} \qquad \text{(A-26)}$$

Through Eqs. (A-22) - (A-26), value of the number of internal elastomer layers, N, can be determined.

- **Minimum Reinforcement Thickness**

The thickness of the reinforcement, h_s, shall satisfy the same standard as in Method A, Eqs. (A-10) and (A-11).
Based on steps above, the design shear force is obtained from Eq. (A-12). The total thickness of bearings can be obtained from Eq. (A-13).

A-5. Additional Design Tips

- For some circumstances, a bearing designed by Method A is larger than the one designed by Method B. Despite the extra size, bearings designed by Method A may prove cheaper since the test requirements are less stringent.
- Horizontal forces (design shear force) applied to the substructure can be minimized by using smallest plan dimensions and maximum height possible. Since rotations were found to use up only a small amount of the compressive capacity, a square bearing may be more appropriate. This will increase the buckling load and allow a larger height bearing[5].
- In practice, minimum thickness for elastomer layer and steel lamination are 5mm and 1.6mm, respectively.

A-6. Review Problem

The bearing problem can be classified broadly as review problems or design problems. In the case of design problems, the required load, displacement capacities and material strengths are given, and the dimensions and reinforcement in elastomeric bearings need to be calculated. In review problems, a bearing is provided, i.e., the dimensions, reinforcement, and material strengths are known, and then the load and displacement capacity are to be determined. Hence, for review problems, we need to check (1) shear and compressive stresses in bearings; and (2) shear displacement capabilities of bearing, according to AASHTO standard specifications for highway bridges[7].

The known parameters for review problems are listed as below:

- The material properties of elastomer: shear modulus (G) and $\bar{k}$.
- The material properties of steel plate: yield strength of the steel plate (F_y) is fatigue limit stress of steel ($(\Delta F)_{TH}$).
- The dimension parameters: h_{cover}, $W \times L$, h_{ri}, h_s.
- The composition of bearing: number of internal elastomer layers *N*.
- Service load (dead load P_{DL}, live load P_{LL})
- The structural displacement requirement at bearing, that is, $\theta_{TL,x}$, $\theta_{TL,z}$ and Δ_s
- Translation fixed condition in *x*, *y* direction

A-6.1. *Review According to the Standard of Design Method A*[12,30,7,5]

Flowchart for the review of bearings by Method A is shown in Fig. A-1. If the result of every check is satisfactory, then the given bearing can meet the practical requirement on the load and displacement capacities according to the AASHTO standard specifications (Method A) for highway bridges. Otherwise, some adjustments are needed.

A-6.2. *Review According to the Standard of Design Method B*[12,30,7,5]

Flowchart for the review of load and displacement capacities of bearings by Method B is shown in Fig. A-2.

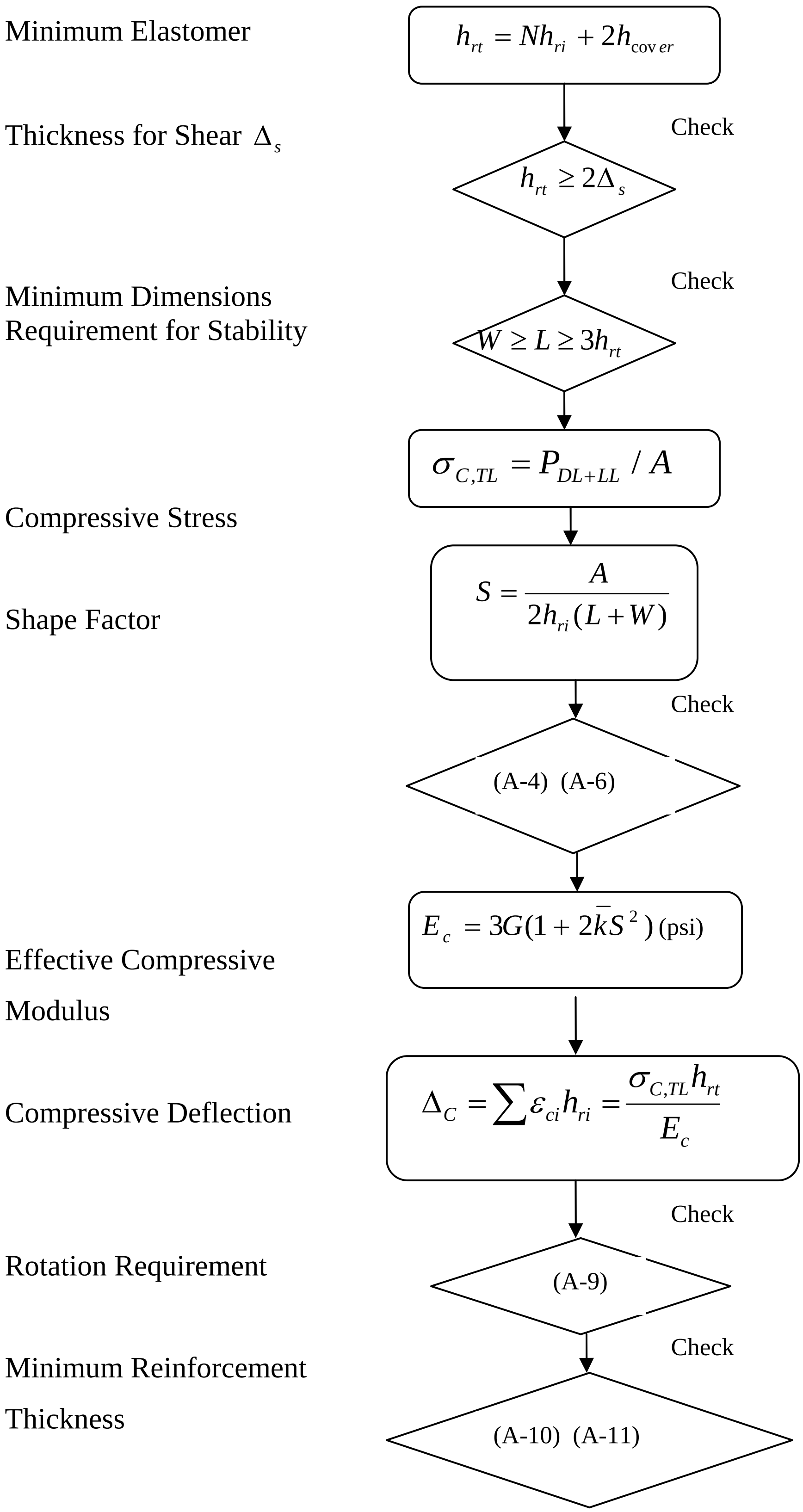

Figure A-1: Flow Chart for Bearing Load and Displacement Capacities Using Method A

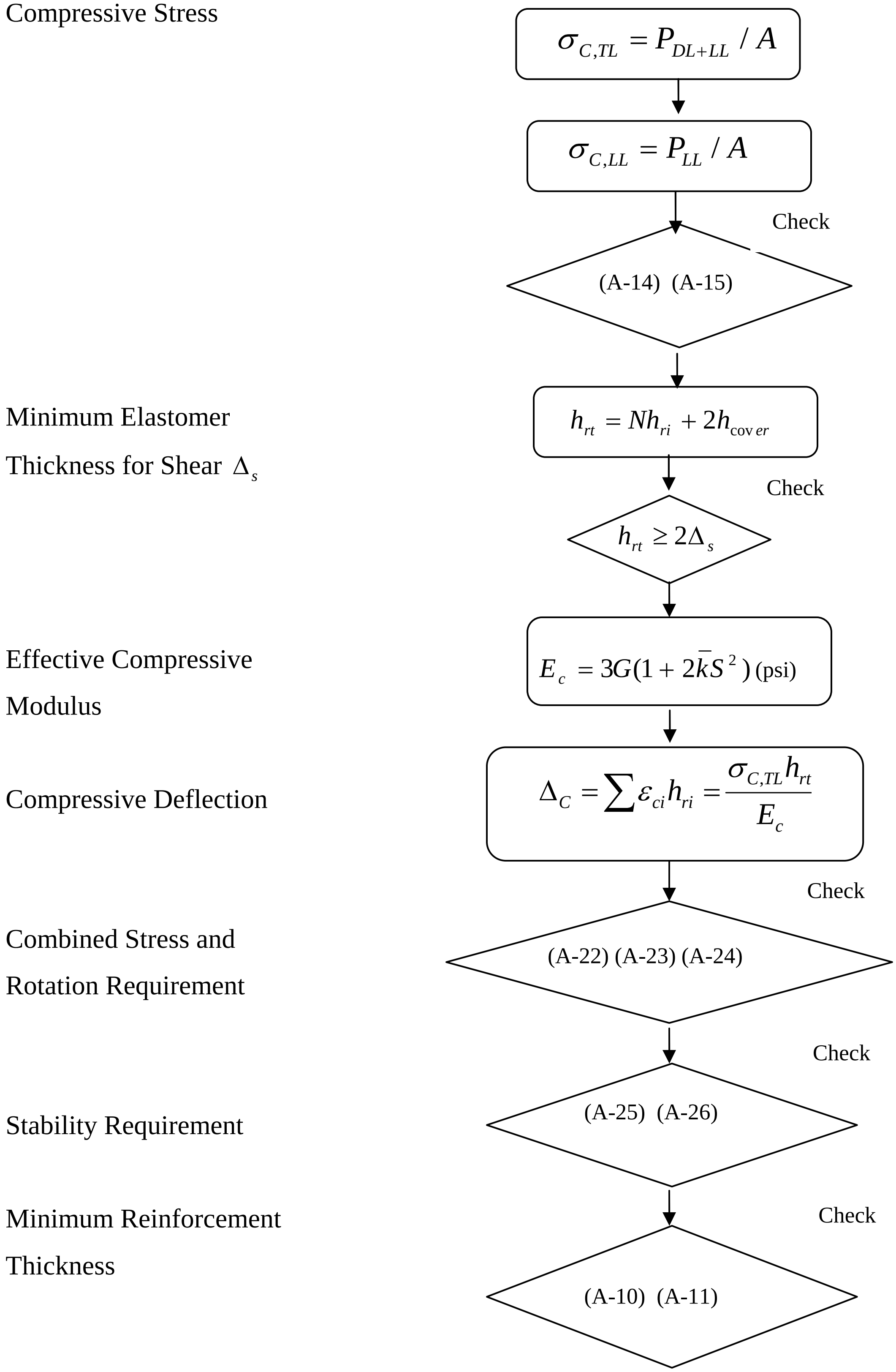

Figure A-2: Flow Chart for Bearing Load and Displacement Capacities Using Method B

A-6.3. *Shear Stress*

- **Design shear force [As per Eq. (A-12)]**

$$H = \frac{GA\Delta_s}{h_{rt}}$$

G: the maximum shear modulus.

- **Design shear stress:**

$$\tau = \frac{G\Delta_s}{h_{rt}} \tag{A-27}$$

- **Maximum shear displacement permitted:**

$$\Delta_s = h_{rt} \times 0.5$$

(A-28)

- **Maximum shear force permitted:**

$$H = GA \times 0.005$$

(A-29)

A-7. Low Temperature Behavior and Acceptance Test of Elastomeric Bearings

In order to ensure satisfactory performance in field, the 3rd phase of the NCHRP Project 10-20 concentrated primarily on the low temperature behavior of the bridge bearing elastomers. The research included collection of existing data, and laboratory tests of elastomer stiffening and crystallization at low temperatures.

A-7.1. *Low Temperature Behavior*

It has long been recognized that elastomers may stiffen dramatically at low temperatures, and sometimes the maximum bridge movement occurs during periods of very low temperature. This results in a corresponding increase in incremental forces, and moments for incremental shear and rotational deformations occur at these low temperatures. This causes shear force to be larger than the bearing design force in the bearing and the structure. The bearing design force is defined as the calculated force induced in the bearing when the bridge superstructure undergoes its maximum design movement using room temperature ($23^0 C$) properties of the elastomer.

The compressive stiffness of a layer of an elastomeric bearing depends on the stiffness of the elastomer and the shape factor, which is an indicator for the degree of restraint provided by the reinforcement[10,11]. A bearing layer with a larger shape factor and higher elastomer stiffness has larger compressive stiffness. Furthermore, an increase in the elastomer stiffness of the plan area of the bearing results in a direct increase in shear force ($H = \frac{GA\Delta_s}{h_{rt}}$) for a given movement. In brief, both the compressive stiffness and shear stiffness increase at the lower temperatures[5].

Based on hardness and compression set tests of the elastomer[6], two types of low temperature stiffening, i.e., crystallization or instantaneous thermal stiffening, have been found. Crystallization is dependent on time and temperature, and it is very sensitive to the elastomer compound. Crystallization occurs after the elastomer has been exposed to low temperature for a period of days or weeks. Instantaneous thermal stiffening occurs very quickly (in a few hours), normally at temperatures well below those that cause crystallization. Elastomers may also reach a brittle state known as the glass transition at very low temperatures. Neoprene crystallizes more rapidly than natural rubber. On the other hand, natural rubber reaches instantaneous thermal stiffening at lower temperatures than most Neoprene compounds[5,31,32].

The elastomer should have low temperature properties that are appropriate for the environment. Otherwise, very large low temperature forces may cause damage to the structure. This potential for damage, combined with the more liberal design provisions for elastomeric bearing design using Method B design procedure illustrates the importance of having an adequate and appropriate low temperature test procedure for elastomeric bridge bearings.

A-7.2. *Acceptance Test for Elastomers at Low Temperature*

The established test methods are used by state bridge engineers to certify that the elastomeric compound provided for bridge bearings is adequate for the climatic requirement of that region. The test apparatus was designed and built and it is used to perform a wide range of low temperature tests on elastomeric bridge bearings.

The tests shall be performed in accordance with the requirements of Tables 18.4.5.1-1 A and B[7]. They are low temperature brittleness test, instantaneous thermal stiffening test, and low temperature crystallization test. Furthermore, the compound shall satisfy all the limits for its grade. The Table 14.6.5.2-2 in Ref.6 specifies the elastomer with the minimum low temperature grade.

Regarding the testing frequency, the three low temperature tests on the elastomer shall be conducted on the material used in each lot of bearings for grades 3, 4, and 5 materials, and the instantaneous thermal stiffening test shall be conducted on material of grades 0 and 2. Low temperature brittleness and crystallization tests are not required for grades 0 and 2 materials, unless especially requested by engineers. For grade 3 material, in lieu of the low temperature crystallization test, the manufacturer may choose to provide certificates from low-temperature crystallization tests performed on identical material within the last year, unless otherwise specified by the Engineer[7].

A-7.3. *Design Requirements for Low Temperature Behavior*

The results of the low temperature tests were combined with an analytical study of temperature conditions in the United States and specific recommendations for the AASHTO Specification were derived[5]. These detailed recommendations have been included in AASHTO Design Specification and Construction Specification[7,30].

For the purpose of bearing design, all bridge sites shall be classified as being in temperature Zones A, B, C, D, or E. Characteristics for each zone are given in Table 14.6.5.2-2 of Ref.6. In the absence of more precise information, Figure 14.6.5.2-2 of Ref.6 may be used as a guide in selecting the zone for a given region.

Bearings shall be made from AASHTO low temperature grades of elastomer. Any of the three design options listed below may be used[30,7]:

- Specify the elastomer with the minimum low temperature grade indicated in Table 14.6.5.2-2 of Ref.6 and determine the shear force transmitted by the bearing as specified in Article 14.5.3.1 of Ref. 6 (Formulas are listed in the Note below) .
- Specify the elastomer with the minimum low temperature grade for use when special force provisions are incorporated in the design, and provide a low friction sliding surface,

in which case the special force provision is that the bridge components shall be designed to withstand twice the design shear force specified in Article 14.5.3.1 of Ref. 6, or

- Specify the elastomer with the minimum low temperature grade for use when special force provisions are incorporated in the design, but do not provide a low friction sliding surface, in which case the components of the bridge shall be designed to resist four times the design shear force specified in Article 14.5.3.1 of Ref. 6.

Note: The design shear force specified in Article 14.5.3.1 of Ref. 6 may induce sliding friction, rolling friction or deformation of a flexible element in the bearing. The force used for design shall be the largest one applicable.

Sliding friction force: $H_m = \mu P_m$ (A-30)

p_m =maximum compressive load

μ =coefficient of friction

The force required to deform an elastomeric element:

$$H_m = G\,A\,\Delta_s\,/h_{rt}$$

(A-31)

Rolling forces shall be determined by test.

APPENDIX B

SENSOR TECHNOLOGY

B-1. Introduction

Recent advances in both sensor design and computer-based data acquisition allow for direct measurements, real time processing and display, and also transmission of data. There are 10 main sensor types currently used in practice: chemical, temperature, strain, biomedical, electrical and magnetic, rotation, vibration, displacement, pressure, and flow sensor. The measurements required for implementing the smart bearing, which have been identified, are: force; strain; displacement; acceleration and temperature. Development of smart bearings requires a careful evaluation of sensors which provide measurements of the required variables over the desired ranges and also provide a desirable level of performance in the long –term when subjected to the environment. This appendix catalogs applications, reference information and suppliers of sensors for force, strain, displacement, acceleration and temperature which have been found suitable for smart bearing application.

B-2. Force Sensors

Implementation of the smart bearing requires an accurate determination of the axial force in the bearing to determine bridge reactions. Conventional force/load sensors are unsuitable for such an application for the following reasons: (a) the magnitude of forces involved would make such sensors physically large, and (b) the cost of such sensors for the required magnitude would be substantial. Recently thin-film tactile force sensing array have been developed and have been patented by Tekscan designs. The sensors consist of two flexible polyester sheets that have strips of electrical conductors deposited on them. A thin silver-based semi-conductive coating is sprayed on the electrical conductors to form an intermediate layer providing an electrical resistance/ conductance between intersecting contacts. The layer's electrical resistance, which changes with applied external force, is of major importance. The two sheets are bonded together creating a sensor with the electrical conductors forming a grid pattern with a sensing cell at each intersection. The sensor provides an array of pressure-sensitive cells. The applied load/force is measured by monitoring the minute changes in current flow at each sensor cell caused by the force. These sensing arrays measure force and pressure distribution between two mating surfaces making it possible to evaluate the location and magnitude of contact pressure. Currently, the system available commercially allows viewing static and dynamic pressures using a two-or three- dimensional computer graphics display in real time. Recordings can be taken at sampling speeds of up to 10 KHz and ASCII files are generated. Sensors are available in almost any size and shape. Details of the pressure measurement system based on the thin film force sensing arrays are provided below.

****

Sensor Name: Dynaforce System
Measurement provided by sensor: Primary measurement is of contact pressure. The total force can be obtained by integrating the pressure.
Measurement Range: Sensors with pressure ranges as low as 0 – 2 Psi (14 kPa) and as high as 0 – 25,000 Psi (175 MPa) have been produced.

** The sensor resolution can be custom designed to fit the analytical requirements of the application's stress range and resolution.
Temperature Range: 15°F to 140°F (-9°C to 60°C)
Hardware Requirement: Thin-Film (0.1mm thick) Tactile Force Sensing Arrays
Vendor/ Manufacturer: Teksan
Approximate Cost: $25,000 (entire system)
Web Address: http://www.teksan.com/
Tel: 617-464-4500 marketing@tekscan.com
****

B-3. Strain Sensors

Strain in a material is a measure of the relative displacement between two material points. Strain allow for assessing the stress in the material, and hence provide an indirect measure of load. The strain gage is a device used for measuring normal strain in a specific direction. There are many kinds of strain gages. For example, some are acoustic, capacitive, inductive, mechanical, optical, piezo-resistive, and semi-conductive, etc. All strain gages depend on the relationship between the strain and certain properties of the material of the sensor, such as electrical resistance, capacitance or inductance. Information about the different types of strain gages available commercially are described below.

B-3.1. *Electrical-Resistance Wire Strain Gages*

The most commonly used strain gage, electric-resistance wire strain gage, is made of a resistor, usually in metal foil form, bonded on an elastic backing. As a resistive elastic unit, it operates on the principle that the change in electrical resistance of wires is a function of applied strain, that is, the change in wires' length. The gage is cemented to the object, so that the gage and object undergo the same normal strain. The resulting change in the electrical resistance of the gage element is measured and converted into strain. Among all strain gages, the electric-resistance wire strain gage has the advantages of lower cost and being an established product. Thus it is the most commonly used type of device while at the same time very accurate and durable.

****
Sensor Name: Transducer Strain Gages
Measurement provided by sensor: Strain
The resulting change in the electrical resistance of the gage element is measured and converted into strain.
Measurement Strain Range: $\pm 2250 \mu\varepsilon$
Temperature Range: with appropriate choice of the adhesive, the usable range in temperature can be as low as -265°C and as high as +400°C.
Hardware Requirement: A wire strain gage is made by a resistor, usually in metal foil form, bonded on an elastic backing.
Vendor/Manufacturer: Vishay Measurements Group
Web address: http://www.blh.de
Tel: 919-365-3800 info@vishaymg.de email@measurementsgroup.com
****

B-3.2. ***Vibrating Wire Strain Gages***

The Vibrating Wire Technology is based on the dependency of a vibrating wire's resonant frequency on its tension. Vibrating wire strain gages commercially available today provide long-term stability, high resistance to water intrusion and lightning damages and the ability to be used with long signal cables. In addition, temperature effects are compensated internally in such gages using thermistor which permit thermal induced stains to be distinguished from load-induced strains. Vibrating wire strain gages are available in different gage lengths ranging from 4 inches to 12 inches, and can be surface mounted or embedded inside the material. These gages are not suitable for dynamic applications.

****

Sensor Name: Vibrating Wire Strain Gage
Measurement provided by sensor: The resulting change in the electrical resistance of the gage element is measured and converted into strain.
Measurement Range: a 3000 microstrain range and 1 microstrain sensitivity.
Temperature: Temperature effects are automatically compensated for when the gages are welded to steel. The thermistor permits real thermal induced strain to be distinguished from load-induced strains.
Hardware Requirement: Based on vibrating wire technology, a vibrating wire strain gage is made by a resistor, usually in metal foil (coil) form, bonded on an elastic backing.
vendor: currently vibrating wire strain gages are marketed by several vendors, like Geokon (www.geokon.com), Roctest (www.roctest.com), and Slope Indicator (www.slopeindicator.com)
****

B-3.3. ***Interferometric Fiber Optic Strain Gauges***

Fiber optic sensor technologies are finding growing application in the area of structural monitoring. The costs for fiber sensors have been dropping steadily due to the rapid advances in communications technologies, and this trend will continue. Further, measurement capabilities and system configurations (such as wavelength multiplexed, quasidistributed sensor arrays) that are not feasible with conventional technologies now are possible with fiber sensors, enabling previously unobtainable information on structures to be acquired.

The phenomenon of the interference of light underlies many high-precision measuring systems and displacement sensors. The use of optical fibers allows making such devices extremely compact and economic. Two basic concepts of fiber optic interferometers are known: Mach-Zehnder and Fabry-Perot interferometers. In Fabry-Perot fiber optic interferometer, the interference occurs at the partially reflecting end face surface of the fiber and an external mirror. The size of the sensitive element based on this principle can be as small as diameter of the fiber, i.e. about 0.1 mm, and the sensitivity can achieve sub-angstrom level. We can use low coherence optical source (which may be even a superluminescent diode). Additionally, this type of interferometer is not sensitive to electro-magnetic interference and can be used in hostile environment.

Fabry-Perot interferometric strain gauges (Figure B-1) have been used to produce self-monitoring structures such as bridges, buildings and roads. Fabry-Perot interferometers can be used to measure strain, force and load, temperature, pressure, linear position and displacement applications. A broadband white light source is conveyed via an optical fiber to two mirrors, representing the strain gauge. As strain, in the form of mechanical, temperature or other forces, is placed on the gauge, the distances between the mirrors change and modulates the optical spectrum. The return signal passes through an optical correlator before reaching a linear CCD array. By detecting the maximum signal strength on the linear array, the system determines the absolute distance between the mirrors and therefore the strain inside the structure.

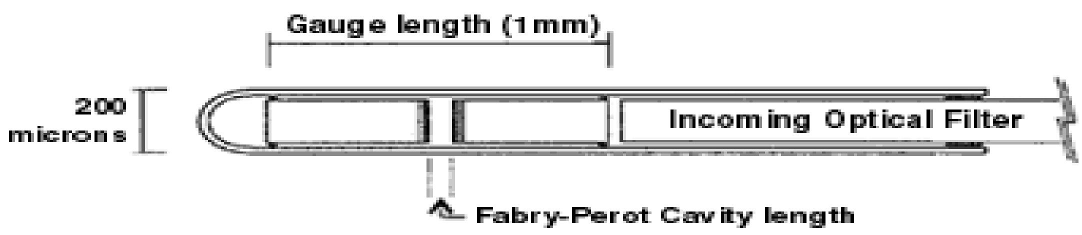

Figure B-1. FISO Fabry-Perot Interferometric Strain Gauges

Several companies and institutions around the world make use of other interferometry, including Michelson Mach-Zehnder and Sagnac interferometers. Fabry-Perot interferometers, however, do not need more than one optical fiber for operation. Other benefits of Fabry-Perot method include absolute values where the existing strain value is not lost by turning the system off, independence of signal strength and the use of multimode fibers, which are easier to incorporate into many mechanical and structural systems.

****

Sensor Name: Interferometric Fiber Optic Sensors
Currently, a 32-channels fiber optic data acquisition system, which allow for continuous monitoring of the long-term behavior of this structure, are available. This field application demonstrates that Fabry-Perot fiber optic sensors are suitable for the short and long-term monitoring of bridge performance.
Measurement provided by sensor: Strain (by Fabry-Perot fiber optic interferometric strain gauges)
A broadband white light source is conveyed via an optical fiber to two mirrors, representing the strain gauge. As strain is placed on the gauge, the distances between the mirrors change and modulate the optical spectrum. The return signal passes through an optical correlator before reaching a linear CCD array. By detecting the maximum signal strength on the linear array, the system determines the absolute distance between the mirrors and therefore the strain inside the structure.
Measurement Strain Range: ±5000$\mu\varepsilon$
The sensitivity can achieve sub-angstrom level, and other ranges are available on request.
Temperature Range: -40°C to +250°C
Operating temperature is adhesive dependent. Installation over 200°C is susceptible to creeping.
Hardware Requirement: Mach-Zehnder or Fabry-Perot fiber optic interferometers
In Fabry-Perot fiber optic interferometer, the interference occurs at the partially reflecting end face surface of the fiber and an external mirror.
Vendor/Manufacturer: FISO Technologies Inc., and Roctest
Web Address: http://www.fiso.com/ and www.roctest.com
Tel: +418-688-8065 info@fiso.com
****

B-4. Displacement Transducers

There are two types of displacement transducer principles: capacitive and inductive (eddy current), which operate on electric and electromagnetic fields, respectively

B-4.1. *Capacitive Displacement Transducers*

The displacement transducer measures the gap between its front face and a suitable target material. The electronics position sensor is built into the unit so it provides a dc output proportional to the gap measurement from a dc supply. Suitable target materials for non-contact displacement measurement using this capacitive technique are all metals, many types of plastic, some glass and anything that contains water or carbon in reasonable levels. A good target has a high relative permittivity and/or low receptivity. Such sensors are not suitable for applications where water may be splashed since water is a suitable target.

****

Sensor Name: Non-Contact Capacitive Displacement Transducer
Measurement provided by sensor: The position sensor is built into the unit. Thus, based on capacitive technique, it provides a dc output proportional to the gap measurement from a dc supply.
Measurement Range: The capacitive transducer available had the disadvantage of a relatively short operating distance (<20mm)
Temperature Range: -25°C to +85°C
Hardware Requirement:
The displacement transducer measures the gap between its front face and a suitable target material. The electronics for the SensaGap position sensor is built into the unit so it provides a dc output proportional to the gap measurement form a dc supply, based on capacitive technique.
Vendor/Manufacturer: RDP Electrosense Inc
Web Address: http://www.rdpe.com/displacement/sensagap/senagap.htm
Tel: 610-469-0850, sale@rdpelectrosense.com
****

B-4.2. *Linear (LVDT) Displacement Transducers*

LVDT stands for Linear Variable Differential Transformer. The basic unit consists of a primary coil and two secondary coils wound on a coil form. A ferromagnetic core links the electromagnetic field of the primary coil to the secondary coils as shown in Figure B-2. Differencing the output of these coils will result in a voltage proportional to the relative movement of the core versus the coils.

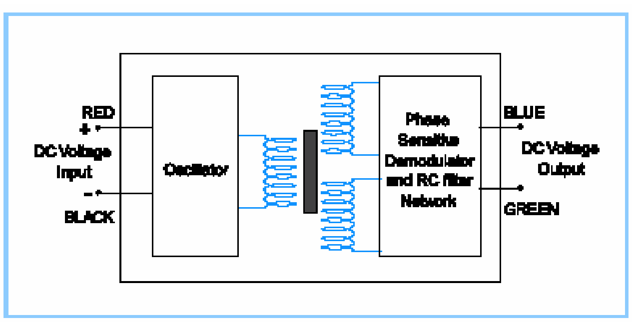

Notes:
1. Polarity of excitation must be observed for proper function. Reversal will not damage the unit.
2. Load Impedance of 50 KOhms minimum required for proper operation.
3. Output polarity will be positive on one side of null, negative on the other side of null.
4. Transducers are calibrated at 24 VDC.
5. Blue lead is more positive with respect to the Green lead when the core is moved toward the lead end.

Figure B-2. Linear (LVDT) Displacement Transducer

LVDTs are currently commercially available in different configurations and for varying ranges of displacement.

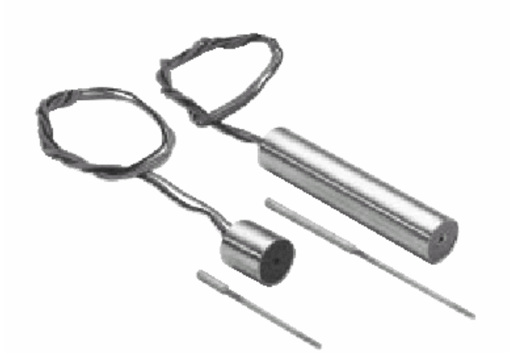

Figure B-3. Typical LVDT in Stainless Steel Construction

****

Sensor Name: Linear (LVDT) Displacement Transducer
Measurement provided by sensor: Displacement
Measurement Range:
Working Range: available from a range ± 0.001 inch to ± 6 inch
Sensitivity = 0.1%
Temperature Range: -65° F to +25° F (-54° C to 121°C)
Vendor/Manufacturer: Trans-Tek Inc, Sensotec, Shaevitz
Web Address: www.transtekinc.com http://www.sensotec.com/
Tel: for Trans-Tek 800-828-3964 or 860-872-8351 Fax: 860-872-4211

****

B-5. Accelerometer

Accelerations are required to obtain the dynamic response of the bearings. Measured acceleration at the bearings provides a means to access the role of elastomeric bearings in the dynamic response of bridge subjected to impact from vehicle loading.

Four accelerometer technologies compete to cover most applications. They are piezoelectric, piezoresistive, capacitive, or MEMS accelerometer types. Piezoelectric accelerometers produce an electrical charge in response to mechanical stress, while piezo-resistives alter resistance in response to stress. These devices don't offer static-load (or DC) response but are suitable for most general-purpose and high shock measurements. Capacitive accelerometers offer true static-load response. They work well for vehicular-suspension testing, which requires mathematical integration to obtain component velocity and position data. Microelectromechanical system (MEMS) sensors feature micromachined silicon mechanical components and integrated support electronics. Early versions used resistive elements. Today's technology favors capacitive sensors to create truly integrated and very small accelerometers, typically packaged in surface-mount ICs. Besides instrumentation applications, tens of millions of MEMS accelerometers see service in automotive air-bag actuators.

Piezoresistive accelerometers are preferable for use in bearing application because of their range and long-term performance.

****

Sensor Name: Accelerometer
Measurement provided by sensor: In response to mechanical stress, the resulting change in the electrical charge, resistance or capacitance of system sensors is measured and converted into Acceleration.
Measurement Range: ± 3*g* to ± 100*g* full sale
Temperature Range: -40°C to +85°C (General working temperature range)
Hardware Requirement:
(1) Piezoelectric accelerometers produce an electrical charge in response to mechanical stress.
(2) Piezoresistive accelerometers alter resistance in response to stress.
(3) Capacitive accelerometers are based on capacitive technique.
Vendor/Manufacturer: PCB Piezotronics Inc, and Endevco Corporation
Web Address: http://www.pcb.com http://www.endevco.com
Tel: 716-684-0001 or 716-684-0987 for PCB
1-800-982-6732 or 1-949-493-8181 for Endevco
****

B-6. TEMPERATURE SENSORS

B-6.1. *Embedded (contact) thermocouple*

Thermocouples are among the easiest temperature sensors to use and obtain and are widely used in science and industry. They are based on the Seebeck effect that occurs in electrical conductors that experience a temperature gradient along their length. Thermocouples are pairs of dissimilar metal wires joined at least at one end, which generate a net thermoelectric voltage between the open pair according to the size of the temperature difference between the ends, the relative Seebeck coefficient of the wire pair and the uniformity of the wire-pair relative Seebeck coefficient.

****

Sensor Name: Thermocouple Temperature Sensor
Measurement provided by sensor: Temperature
Thermocouple Temperature Sensor is based on the Seebeck effect. The temperature is measured by detecting the generated net thermoelectric voltage.
Measurement Range: over a range of 1800^{o} C to well below zero
Vendor/Manufacturer: Several vendors supply thermocouple temperature sensors.
****

B-6.2. *Infrared Sensors (non-contact)*

Infrared radiation thermometers measure temperature without contact. The principle of an infrared sensor is based upon the adsorption of the infrared light at a specific wavelength. Radiation thermometers can be very accurate and precise. Since a radiation thermometer does not contact the object it is measuring, it does not need to be at the same temperature, thus, it can, in theory, measure very rapidly, measure distant objects, measure moving objects, measure very high temperatures, not interfere with the object's temperature distribution and many more very unique things beyond the limits of, and often competitive with (for accuracy), contact temperature sensors. (It's not easy to measure surface temperature of objects accurately, even with thermocouples or other contact sensors. It’s very difficult to do it when the object is moving or is above the melting temperature of the sensor materials or both) They are the devices, which enable the International Temperature Scale of 1990 at and above the freezing point of silver (961.78°C) to be realized and subsequently defined. Radiation thermometers are often used when nothing else can or will easily provide an accurate temperature measurement. It can be very difficult to prove the error in a radiation thermometer measurement and, conversely, almost equally difficult to prove that the device is measuring accurately.

****

Sensor Name: Infrared Temperature Sensor
Vendor/Manufacturer: available commercially
Measurement provided by sensor: Temperature
Measurement Range: -20°C to +250°C
Hardware Requirement: Infrared radiation thermometers
****